NORTHWESTERN UNIVERSITY

Rare Schizophrenia-Associated Kalirin Variants: Possible Mechanistic Links to Cortical Neuronal Pathology

A DISSERTATION

SUBMITTED TO THE GRADUATE SCHOOL

IN PARTIAL FULFILLMENT OF THE REQUIREMENTS

for the degree

DOCTOR OF PHILOSOPHY

Field of Neuroscience

By

Theron Andrew Russell

EVANSTON, ILLINOIS

September 2018

ABSTRACT

Mounting evidence indicates that known schizophrenia susceptibility genes regulate dendritic spines supports the model that perturbations in the molecular network underlying spine plasticity are crucially involved in the pathogenesis of schizophrenia. The Rac1- and RhoA-guanine nucleotide exchange factor (GEF) kalirin is critical for spine morphogenesis on cortical pyramidal neurons, and postmortem studies have revealed altered kalirin expression in schizophrenia patients. Here I sought to identify rare missense single nucleotide variants (SNVs) in the *KALRN* gene region that encodes one of its gene product's catalytic domains, and identified one in a schizophrenia patient and his sibling with major depressive disorder. The D1338N substitution significantly diminished the protein's ability catalyze the activation of Rac1. Contrary to wildtype kalirin-7, kalirin-7-D1338N failed to increase spine size and density. Both subjects carrying the SNV displayed reduced cortical volume in the superior temporal sulcus (STS), a region implicated in schizophrenia. Consistent with this, mice with reduced kalirin expression showed reduced neuropil volume in the rodent homolog of the STS. These data suggest that single amino acid changes in proteins involved in dendritic spine function can have significant effects on the structure and function of the cerebral cortex. Following this investigation, I turned my attention to another missense SNV, kalirin-9-P2255T, which displays a penetrance greatly exceeds that of previously identified schizophrenia-associated SNVs. Overexpression of kalirin-9-P2255T leads to diminished basal dendritic branching and dendritic spine size in cultured primary cortical pyramidal neurons, as compared to wildtype kalirin-9. The P2255T SNV directly affected kalirin-9 protein function, leading to increased RhoA activation, but had no effect on Rac1. Remarkably, consistent with human postmortem findings, I found that kalirin-9-P2255T protein levels were higher than those of wildtype kalirin-9. This increase was due to increased mRNA stability of the

kalirin-9-P2255T transcript without changes to protein stability, with this SNV predicted to alter mRNA structure. When analyzed together, increased intrinsic RhoA-GEF catalytic activity combined with increased mRNA expression lead to an even greater net activation of RhoA, a protein known to negatively impact dendrites and spines. Taken together, my data reveal a novel mechanism for disease-associated SNVs and provide a platform for modeling morphological changes in mental disorders.

TABLE OF CONTENTS

LIST OF FIGURES

CHAPTER 1: Introduction

1.1: Features of schizophrenia

Schizophrenia is a behaviorally and pathophysiologically complex disorder that affects 0.5-1% of the world's population, with symptoms developing during late adolescence or early adulthood (Bromet & Fennig, 1999; Sham, MacLean, & Kendler, 1994). Although the clinical presentation of schizophrenia can vary, the syndrome is generally characterized by three classes of symptoms: positive symptoms, which include delusions, hallucinations, and a disorganization of thought and speech; negative symptoms, such as affective flattening, anhedonia, alogia, and social withdrawal; and cognitive symptoms, encompassing deficits in executive function, attention, and working memory. In addition to the psychological impact of schizophrenia, patients also have an increase in mortality, dying 12-15 years earlier than the general population (Saha, Chant, & McGrath, 2007). Thus, there is an urgent need to precisely identify the causal factors of schizophrenia to facilitate the development of effective treatments for the disorder.

Although psychosocial interventions are of value in patients for whom psychosis is in remission, pharmacotherapy remains are the foundation of schizophrenia symptom management. The first drugs used for treating schizophrenia, known as first-generation antipsychotics, have been used since the 1950s to treat the positive psychotic symptoms of the disease. Unfortunately, these drugs do little to ameliorate the negative and cognitive symptoms and can cause extrapyramidal side effects. The development of a second generation of antipsychotics, the atypical antipsychotics, allowed for a reduction many of the unwanted side effects but still have little therapeutic advantage over the first-generation antipsychotics (Lieberman et al., 2005). Thus, there is an ongoing need to identify more efficacious therapeutics for schizophrenia patients, particularly with regard to

treating cognitive impairments. Cognitive deterioration often precedes the development of psychosis (Caspi et al., 2003; P. Jones, Rodgers, Murray, & Marmot, 1994) and is the most accurate predictor of clinical outcome (Green, 1996). Cognitive symptoms are relatively stable over time, remain resistant to current treatments, and continue to be present even after psychosis remission (Albus et al., 2002; Keefe et al., 2007). However, for advances in the treatment of cognitive symptoms to occur, researchers must reach a clearer understanding of how affected macroanatomical structural changes, abnormalities in neuronal morphology, and alterations of molecular pathways shape these symptoms.

Postmortem studies of the brains of schizophrenia patients have revealed that one of the defining neuropathological features of schizophrenia is gray matter loss (Selemon & Goldman-Rakic, 1999; Thompson et al., 2001; Vita, De Peri, Deste, & Sacchetti, 2012). These studies have been corroborated by structural magnetic resonance imaging of patient brains, which consistently indicate a thinning of the frontal and temporal cortices (Casanova, 1997; Harvey et al., 1993; Suddath et al., 1989; Zipursky, Lim, Sullivan, Brown, & Pfefferbaum, 1992). Many of the regions with the highest indices of gray matter loss are also associated with cognitive functions that are impaired in the disorder. For example, the dorsolateral prefrontal cortex is critical for working memory and executive function, and schizophrenic individuals show reduced activity of this region during working memory tasks (Weinberger, Berman, & Zec, 1986). Reductions in hippocampal volume have also been reported and could contribute to deficits in verbal declarative memory and spatial learning observed in schizophrenia patients (Kolomeets, Orlovskaya, Rachmanova, & Uranova, 2005; Steen, Mull, McClure, Hamer, & Lieberman, 2006). Importantly, these reductions in volume are not due to neuronal death, as schizophrenia patient brains show normal numbers of

neurons (Pakkenberg, 1993). Given that the cell density in patient brains is increased, it has been hypothesized that a reduction in soma size and neuropil volume is responsible for the overall volumetric decrease (Goldman-Rakic & Selemon, 1997). Thus, factors and processes involved in the development and maintenance of the neuropil may be involved in the development of schizophrenia.

Schizophrenia is a multifactorial neurodevelopmental disorder caused by a combination of genetic and environmental factors. Although no single environmental cause is known to cause schizophrenia, obstetric complications, prenatal nutritional deficiencies, maternal infection, and other prenatal stressors are known risk factors (Bayer, Falkai, & Maier, 1999; Maynard, Sikich, Lieberman, & LaMantia, 2001; Owen, O'Donovan, Thapar, & Craddock, 2011; Walker, Kestler, Bollini, & Hochman, 2004). Although heritability of schizophrenia has been estimated at 80%, its genetic architecture is highly complex, including common variants with very small effects and relatively rare copy number variants with large effect sizes (Gejman, Sanders, & Duan, 2010; Rutkowski et al., 2016). Such complexity greatly exacerbates the challenge of developing effective clinical treatments. Rare genetic alterations (with minor allele frequency, MAF < 0.01-0.05), some occurring in only one family, including CNVs, truncations, missense, and nonsense mutations, might account for an important fraction of the "missing heritability" in schizophrenia (Myers et al., 2011; Sebat, Levy, & McCarthy, 2009). While many CNVs seem highly penetrant perhaps due to gene loss, it is estimated that ~20% of missense point mutations result in a complete loss of function and ~53% have mildly deleterious effects (Kryukov, Pennacchio, & Sunyaev, 2007). The presence of one or two highly penetrant single variants or the accumulation of several mildly

deleterious variants in an individual's genome could thus predispose the carrier to disease. This hypothesis is strongly supported by findings of rare mutations in a small number of families, and in *NLGN3-4X* and *SHANK3* in autism (Buxbaum, 2009). Because such mutations are estimated to impair protein function, many are expected to lead to cellular and brain circuit alterations, and thus influence clinical measures in patients.

1.2: Regulation of dendritic spines and their role in schizophrenia

Dendritic spines, mushroom-shaped protrusions of dendrites, are the sites of most excitatory synapses on pyramidal neurons in the mammalian forebrain (Fiala, Spacek, & Harris, 2002; Harris, 1999). Spine plasticity contributes to the remodeling of neural circuits that is crucial for postnatal cognitive development (Alvarez & Sabatini, 2007; Petrak, Harris, & Kirov, 2005). Structural plasticity parallels the changes in glutamate receptor content that underlie functional plasticity, as spine size and density tend to increase during long-term potentiation and decrease with long-term depression (Feldman 2009, Rochefort & Konnerth 2012). Additionally, morphological changes have been observed *in vivo* following animals' exposure to various environmental and social stimuli (Lamprecht & LeDoux, 2004). Importantly, altered dendritic spine size and density are consistently observed in the cortices and hippocampi of the postmortem brains of schizophrenia, Alzheimer's disease, Fragile X syndrome, and autism spectrum disorder patients (Glantz & Lewis, 2000; Hutsler & Zhang, 2010; Irwin, Galvez, & Greenough, 2000; Mavroudis et al., 2011). At the biochemical level, these structural changes are generated by changes in actin cytoskeleton structure, as well as altered patterns of endocytosis and exocytosis, but the exact mechanisms of how these processes are regulated are unclear. Therefore, it is imperative to tease out the links

between post-synaptic receptors and adhesion molecules and their ultimate effects on actin reorganization in particular, and spine dynamics in general.

Among the more well-studied factors involved in spine formation, stability, and plasticity are the Rho family of small GTPases, including RhoA and Rac1 (Duman, Mulherkar, Tu, J, & Tolias, 2015; Tolias, Duman, & Um, 2011). These small GTPases serve as "molecular switches", as they oscillate between an active GTP-bound state and an inactive GDP-bound state as a result of their intrinsic GTPase activity. GTPase activity is regulated by several classes of proteins, including guanine nucleotide exchange factors (GEFs), which activate GTPases by facilitating the exchange of GDP for GTP; GTPase-activating proteins (GAPs), which inactivate GTPases by hydrolyzing bound GTP; and guanine dissociation inhibitors (GDIs), which sequester inactive GTPases from GEFs that could potentially activate them (Cherfils & Zeghouf, 2013). The activity of GEFs and GAPs are regulated in turn by multiple extracellular signaling pathways, such as those activated by glutamate, neurotrophic factors, and synaptic cell adhesion molecules (Lai & Ip, 2013).

When activated, GTPases can bind various effector proteins, which in turn induce cytoskeletal changes. Through its activation of synaptic proteins such as p21-associated kinase (PAK) and members of the Wiskott-Aldrich syndrome protein family (e.g., WAVE1 and N-WASP), Rac1 initiates a cascade of events leading to decreased actin depolymerization, increased filament nucleation, and increased filament extension (Soderling et al., 2007; Wegner et al., 2008). The net effect of this activity is to promote both the formation of new spines and the stability of existing spines. RhoA activates ROCK, which in turn activates LIMK and inhibits cofilin, thereby

also promoting actin polymerization (Meng et al., 2002). Complicating the situation however, is the observation that Rac1-effectors are capable of inhibiting RhoA activation, and vice versa (Guilluy, Garcia-Mata, & Burridge, 2011). Recently, the spatial and temporal regulation of these GTPases' oscillations between active and inactive states was shown to coordinate distinct forms of excitatory synaptic plasticity (Hedrick et al., 2016). Thus, it is ultimately the balance of activation, abundance, and spatiotemporal pattern of GTPase and effector activation which ultimately determine how the cytoskeleton is modulated within a given dendrite or spine (Duman et al., 2015).

During normal development, cortical pyramidal neurons undergo a period of synaptic pruning during adolescence to refine connections before reaching a steady state level in adulthood (Huttenlocher, 1979). This pruning is exaggerated in schizophrenia, and diminished synaptic density, along with less extensive dendritic arborization and smaller pyramidal neuron soma size, is thought to be one of the cellular morphological changes responsible for the decreased cortical gray matter observed in patients (Glantz & Lewis, 2000; Glausier & Lewis, 2013; Selemon, Rajkowska, & Goldman-Rakic, 1998). Postmortem studies have shown brain regions with the highest indices of gray matter loss also have noticeable reductions in spine density, and many of these regions have been associated with perturbed function in schizophrenia patients. For example, the dorsolateral prefrontal cortex (DLPFC) is critical for working memory function and schizophrenic individuals show reduced activity of this region during working memory tasks. Spine loss in the DLPFC has been reproducibly reported, particularly in layer 3 neurons (Glantz & Lewis, 2000), and a profound reduction in spine density on pyramidal neurons of the primary auditory cortex has also been observed (MacDonald et al., 2017; Sweet, Henteleff, Zhang,

Sampson, & Lewis, 2009). Other postmortem analyses of brains from schizophrenia patients also demonstrate a reduction in the density of cortical dendritic spines in the anterior cingulate cortex, and the superior temporal gyrus (Hill, Hashimoto, & Lewis, 2006; Lewis & Sweet, 2009). Reduced spine density on subicular and CA3 dendrites have also been consistently reported in schizophrenic patients (Kolomeets et al., 2005; Steen et al., 2006). Decreased dendritic complexity may also contribute to schizophrenia etiology and symptomatology, as reductions in dendrite length have also been found in layer 3 and layer 5 of the prefrontal cortex (Broadbelt, Byne, & Jones, 2002; Kalus, Muller, Zuschratter, & Senitz, 2000; Konopaske, Lange, Coyle, & Benes, 2014).

Many schizophrenia risk genes encode proteins that affect synapse structure and function (Glessner et al., 2010; J. Hall, Trent, Thomas, O'Donovan, & Owen, 2015). Enormous progress has been made over the past decade in uncovering the molecular networks that control spine plasticity, and several major schizophrenia risk genes, such as *NRG1*, *ERBB4*, *DISC1*, and *DTNBP1*, as well as the schizophrenia-associated 15q11-13 microduplication, appear to regulate spine plasticity (Isshiki et al., 2014; Ito et al., 2010; Marshall et al., 2017; Penzes, Cahill, Jones, VanLeeuwen, & Woolfrey, 2011; M. Wang et al., 2017). Conversely, many known regulators of spine plasticity have been associated with schizophrenia, through genetic association or candidate gene studies (Kushima et al., 2012), copy number variant analysis (Fromer et al., 2014; Purcell et al., 2014), or postmortem neuropathology (Hill et al., 2006). Taken together, these findings suggest spine pathology, particularly in pyramidal neurons of the cortex and hippocampus, may contribute to the diverse clinical symptoms of schizophrenia.

1.3: Kalirin: a regulator of neuronal morphology with links to schizophrenia

One GEF that has gained attention for its potential link to schizophrenia and other psychiatric disorders, such as AD and attention-deficit/hyperactivity disorder, is kalirin (Penzes et al., 2011; Remmers, Sweet, & Penzes, 2014). The *KALRN* gene encodes multiple protein isoforms, kalirin-7, -9, and -12 being the most abundant, which include various combinations of protein-protein interaction and enzymatic domains. Notably, kalirin-7 has a single Rac1-GEF domain and a PDZ-binding domain; kalirin-9 and the longer kalirin-12 lack this PDZ-binding domain but contain an additional GEF domain capable of activating RhoA (Penzes, Johnson, Kambampati, Mains, & Eipper, 2001). In postmortem studies, kalirin mRNA and kalirin-7 protein levels were found to be reduced in the prefrontal cortex of schizophrenia patients (Hill et al., 2006; Rubio, Haroutunian, & Meador-Woodruff, 2012). In contrast, kalirin-9 has been shown to be upregulated in auditory cortex in schizophrenia (Deo et al., 2012). Resequencing and association analysis have also identified several rare missense mutations in the human *KALRN* gene have been identified and were shown to be enriched in patients with schizophrenia (Kushima et al., 2012).

In vitro studies using antibodies targeted to specific kalirin domains, kalirin-7, -9, and -12 have shown that these distinct isoforms have distinct localization in cultured neurons (Johnson, Penzes, Eipper, & Mains, 2000). Kalirin-7 in particular is enriched in dendritic spines, where it colocalizes with PSD95. Kalirin-7 overexpression in cultured cortical pyramidal neurons increases both spine density and area, whereas RNAi-mediated knockdown of kalirin in cultured neurons, as well as incubation of neurons with a peptide that competes with PSD95 for kalirin-7 binding, results in both decreased spine density and area (Xie et al., 2007). Kalirin-7 is also required for NMDA

receptor-dependent structural plasticity and concomitant increases in synaptic AMPA receptor expression (Xie, Cahill, & Penzes, 2010; Xie et al., 2007). On the other hand, kalirin-9 is expressed primarily in dendrites, and in vitro overexpression of this isoform leads to an attenuation of dendritic branching and increase in spine size and density (Deo et al., 2012). Thus, alternate splicing of the *KALRN* gene gives rise to protein products with differential localization and catalytic activity, allowing for complex regulation of cytoskeletal changes.

Mice that are homozygous for a *Kalrn* null allele exhibit behavioral deficits related to schizophrenia, as well as reduced dendritic length and complexity *in vivo* (Xie et al., 2010). Kalirin-KO mice also exhibit a reduction in hippocampal cell number and area and a thinning of the frontal cortex (Xie et al., 2010; Xie et al., 2011). Cultured neurons from these animals fail to undergo the usual increases in spine size and AMPA receptor content seen in wildtype neurons following chemically induced long term potentiation. Additionally, Kalirin-KO knockout mice display reduced dendritic spine density on cortical pyramidal neurons at 12 weeks of age, but not at three weeks of age (Cahill et al., 2009). Intriguingly, this age dependent spine loss resembles the time course of the progression of schizophrenia symptomatology. Furthermore, these morphological and macroanatomical changes correlate with deficits in cognitive tasks known to engage the cortex and hippocampus, including working memory as assessed by the Morris water maze and Y-maze; contextual and cued fear conditioning; and social recognition (Cahill et al., 2009; Vanleeuwen & Penzes, 2012; Xie et al., 2011). A second knockout mouse that lacks only the expression of the kalirin-7 isoform has been developed, and while some of the behavioral and neuronal phenotypes in these animals are distinct from those in the aforementioned knockout, they too show spine dysfunction (Ma et al., 2012; Ma et al., 2008).

Although most studies on kalirin function have focused on its regulation of the actin cytoskeleton via its Rho-GEF activity, several studies suggest an important yet underexplored role of kalirin in postsynaptic membrane trafficking. These studies revealed interactions of kalirin isoforms with several important trafficking proteins, namely Arf6, sorting nexins SNX1 and 2 (SNX1/2), and dynamin-1 and 2. Arf6 is a small GTPase regulator of membrane traffic from recycling endosomes to the plasma membrane and of clathrin-independent endocytosis (Donaldson & Jackson, 2011). In a yeast 2-hybrid screen, Arf6 was shown to interact with the fifth spectrin repeat of kalirin (Koo, Eipper, & Donaldson, 2007). Using non-neuronal cells and overexpressed proteins, Arf6 was shown to modulate kalirin's localization and Rac1 activation. The spectrin region of kalirin has been shown to interact in a yeast 2-hybrid system with sorting nexins (SNX) 1 and 2, which are involved in several steps of the endocytic pathway (Cullen & Korswagen, 2011), and overexpression of SNX1/2 affected kalirin's localization and morphogenic activity in epithelial cells (Prosser, Tran, Schooley, Wendland, & Ngsee, 2010). Dynamin is a GTPase that regulates the scission of vesicles from membranes during endocytosis and at the Golgi apparatus (Gonzalez-Jamett et al., 2013). The IgFn domain of kalirin-12 has been shown to interact with dynamin-2, and overexpression of kalirin-12 or its IgFn domain disrupted dynamin self-assembly and clathrin-mediated transferrin endocytosis in cultured cells (Xin, Rabiner, Mains, & Eipper, 2009). The roles of these interactions in dendrites and synapses of mature pyramidal neurons, and how they may contribute to schizophrenia neuropathology have not been examined. However, trafficking of glutamate receptors through the postsynaptic density, extrasynaptic plasma membrane, and endomembrane system are crucial steps linking structural plasticity to functional plasticity (Henley & Wilkinson, 2016; Pick & Ziff, 2018), and kalirin may play a critical role in

coordinating these processes.

It has previously been shown that kalirin-7 interacts with the schizophrenia risk factor Disrupted in Schizophrenia 1 (DISC1) (Hayashi-Takagi et al., 2010), and that it is a necessary component of pathways downstream of both NRG1/ERBB4 and 5-HT2A serotonin receptor signaling (Cahill et al., 2013; K. A. Jones et al., 2009). *DISC1* variants associated with schizophrenia correlate with reduced cortical thickness in several regions independent of psychiatric diagnosis (Brauns et al., 2011; Cannon et al., 2005; Carless et al., 2011). Knockdown of DISC1 in cultured cortical neurons also results in diminished dendritic spine number (Hayashi-Takagi et al., 2010), and frontal cortex pyramidal neurons in mice carrying *Disc1* missense variants or truncations display reduced spine number and dendrite length than those in wildtypes (Lee et al., 2011; Lepagnol-Bestel, Kvajo, Karayiorgou, Simonneau, & Gogos, 2013). Similarly, patients carrying a schizophrenia-associated minor *NRG1* allele have reduced superior temporal gyrus volumes as compared with patients carrying the major allele (Tosato et al., 2012), and mice lacking CNS expression of *Erbb2* and *Erbb4* exhibit reduced dendritic spine density in frontal cortex pyramidal neurons (Barros et al., 2009). These effects of NRG1/ErbB signaling are dependent on kalirin-7, which is phosphorylated by the ErbB effector Fyn kinase (Cahill et al., 2013). Furthermore, kalirin-7 has been shown to be essential for 5- HT2A receptor-induced dendritic spine growth (K. A. Jones et al., 2009). Antagonism of the 5-HT2A receptor is considered to be an important mechanism of the action of atypical antipsychotic drugs (Meltzer, Massey, & Horiguchi, 2012), and schizophrenic patients consistently exhibit decreased levels of these receptors in several cortical regions (Dean, 2009). Finally, PAK family members have also been shown to be dysregulated in several psychiatric disorders. Missense mutations in PAK3 (Morrow, Kane,

Goff, & Walsh, 2008) and microdeletions in PAK2 (Mulle et al., 2010) have been associated with schizophrenia and intellectual disability, while phosphorylated PAK1 protein is decreased in the cortex of schizophrenia patients (Rubio et al., 2012).

Consequently, the research described below was performed with the aim of disentangling the relationships between the genetic bases for schizophrenia, how genetic risk factors for schizophrenia might impinge upon neuronal morphology in a manner similar to the neuropathological phenotypes associated with the disorder, and whether genetic variants in the *KALRN* gene affecting protein function might be involved in these processes. While the data do not definitively support a definitive causal relationship between rare *KALRN* coding variants and the exact changes in neuronal structure which are thought to give rise to schizophrenia, they do not rule out the possibility. Perhaps more importantly, the experimental program used in this research, utilizing a combination of human genetics, biochemistry, cell biology, and structural imaging of patient brains, represents a useful model for the functional validation of the growing list of schizophrenia risk genes identified by statistical geneticists.

CHAPTER 2: A Sequence Variant in Human *KALRN* Impairs Protein Function and Coincides with Reduced Cortical Thickness

2.1: Background

Abnormal synaptic connectivity is a well-established characteristic of several psychiatric disorders, including schizophrenia, but the exact molecular mechanisms underlying synaptic pathogenesis are not known (Fiala et al., 2002; Penzes et al., 2011). Because dendrites and spines make up a significant fraction of the cortical neuropil, it has been hypothesized that changes in dendrite and spine number and morphology may lead to alterations in cortical thickness measures, a finding reported in several mental disorders, including schizophrenia (Bennett, 2011). The Rac-GEF kalirin-7 has been identified as playing a critical role in spine morphogenesis, and it has been suggested that it may be associated with increased psychiatric risk (Penzes et al., 2011; Penzes & Jones, 2008). Thus, we hypothesized that naturally occurring variants of the *KALRN* gene might alter neuronal morphology in such a manner as to result in either cortical thinning or schizophrenia symptomatology.

Recent large-scale studies revealed that rare sequence variants, such as copy number variations and exonic mutations in glutamatergic synaptic plasticity genes are enriched in subjects with schizophrenia (Fromer et al., 2014; Purcell et al., 2014). However, functional analyses of such sequence variants, especially exonic mutations, present in human subjects in synaptic plasticity genes have not been extensively performed. In addition, the relationship between such molecular and cellular variations and macroscopic brain morphometric phenotypes has not been examined. As an initial step in this direction, we sought to identify coding and potentially functionally important variants in *KALRN* in human subjects, assess the functional impact of such variations, and explore neuromorphometric parameters in carrier subjects. We thus sequenced specifically

in the region that codes for the kalirin protein's Rac1-GEF catalytic domain. We identified one such variant which significantly impaired protein function and neuronal morphology. Interestingly, the subjects carrying this variant displayed reduced cortical thickness in the caudal portion of the superior temporal sulcus. Consistent with this, mice lacking the *kalrn* gene show reduced cortical thickness, suggesting a potential link between molecular and cellular alterations and macroscopic neuromorphological phenotypes.

2.2: Identification of KALRN sequence variants

We screened for missense sequence variants in exons 23-28 of human *KALRN* (Figure 1A), which encode the Dbl homology (DH) portion of its gene products' DHPH1 Rac1-GEF enzymatic domain, in a cohort of well-characterized schizophrenia subjects. The DHPH1 domain has previously been shown to be sufficient to induce Rac1-dependent morphological changes in both heterologous cells and neurons (Penzes et al., 2001); therefore, we reasoned that missense variants in the region coding for it would be more likely to have functional consequences. Sequencing and automated indel/SNP analysis of these exons led to the identification of 15 variants. Eleven of these were intronic, and three resulted in a synonymous codon (Table 1). One rare coding variant, NC_000003.12:g.124462620G>A (NP_001019831.2:p.D1338N), located in the Rac1-GEF domain of *KALRN* was identified in a single subject with schizophrenia (KAL-SCZ) (Figure 1B; Table 1). This initial screen was followed by a second screen of exon 25 for the variant in siblings and non-diseased controls (Table 2). The only carrier for the variant identified in this screen was a sibling of KAL-SCZ (KAL-SIB), who while not schizophrenic, had been diagnosed with major depressive disorder

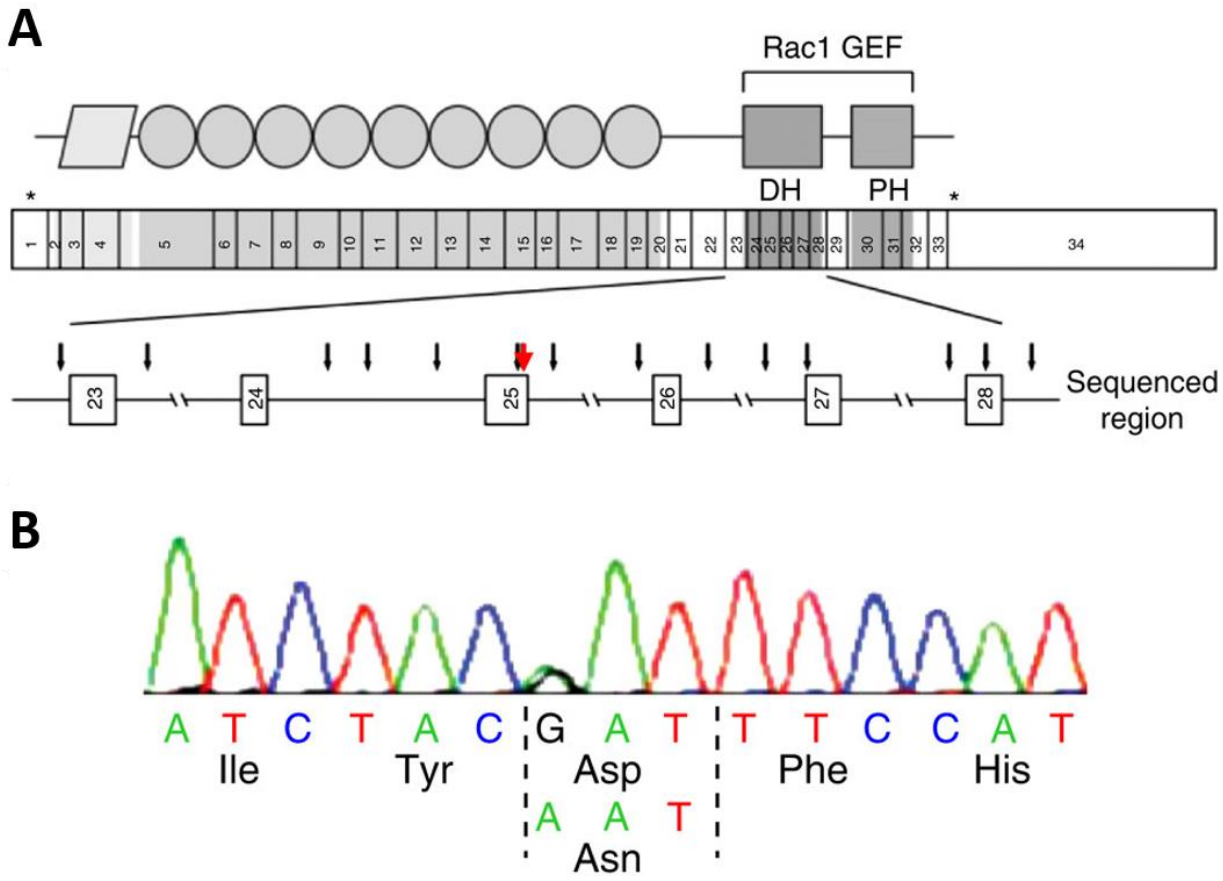

Figure 1. Identification of the *KALRN* variant coding for kalirin-7 p.D1338N. (**A**) Schematic of the kalirin-7 protein (top), mRNA (middle), and the genomic regions that were sequenced. The catalytic Rac1-GEF domain, composed of Dbl-homology (DH) and pleckstrin-homology (PH) domains, is indicated. Fifteen distinct silent and intronic variants identified among 127 patients are denoted by black arrows, and the SNP leading to the p.D1338N variant is denoted by a red arrow. (**B**) Chromatogram illustrating that KAL-SCZ is heterozygous for the minor allele (NC_000003.12:g.124462620G>A) responsible for the kalirin-7 coding variant. The chromatogram from KAL-SIB showed a similar result.

Table 1: *KALRN* coding variants identified in schizophrenia cohort

Exon sequenced (with flanking intronic regions)	dbSNP accession #	NC_000003.12 reference sequence position	Adjacent 5' sequence	Reference base	SNP base	Adjacent 3' sequence	Functional consequence	# carrying SNP/127 patients	
								1 copy	2 copies
23	not available	124456563	AGTGAGTTGC	T	C	TTCCCAAAGC	intron variant	1	0
23	rs113815859	124456818	CTTAATATGT	T	A	CTCATGGCCA	intron variant	1	0
24	rs191254766	124462121	ATAATTACAT	G	A	AGAGTTTAAA	intron variant	1	0
24	rs80214093	124462234	ATGACACAGT	C	T	AGTGAACTTA	intron variant	1	0
25	rs535121	124462414	AAACTCTGCA	C	T	GCATTTACAG	intron variant	38	3
25	rs2289839	124462607	TTGGCAACAT	C	T	CAAGAGATCT	synonymous codon	10	0
25	rs139954729	124462620	AGAGATCTAC	G	A	ATTTCCATAA	missense	1	0
25	rs78944687	124462707	CAAGAAGTGG	A	G	TCAAAGGCGA	intron variant	2	0
26	rs141660253	124474625	GGTCAGCTGC	A	T	CAGAGGTGTC	intron variant	2	0
26	not available	124474811	GACTGGAGTC	A	G	TTGCCAGTCT	intron variant	2	0
27	rs572145	124477140	TAGACACTGG	C	T	GTCTGAGGGT	intron variant	2	0
27	rs2289843	124477247	CTTTTTAGGC	A	T	GACAAATTTC	synonymous codon	14	1
28	rs111967106	124482764	CACACATGCA	C	G	ACACCCCTCT	intron variant	1	0
28	rs61740058	124482852	TCTCTTCCTA	C	T	CTAATTAAGC	synonymous codon	7	1
28	rs71332734	124482977	GGCCCCTAAG	G	A	ATAGGAATGC	intron variant	1	0

Table 2: *KALRN* coding variants identified in siblings and controls

Exon sequenced (with flanking intronic regions)	dbSNP accession #	NC_000003.12 reference sequence position	Adjacent 5' sequence	Reference base	SNP base	Adjacent 3' sequence	Functional consequence	# carrying SNP/238 siblings and controls: 1 copy	# carrying SNP/238 siblings and controls: 2 copies
25	not available	124462298	CACACATTTA	A	G	TAAATGACAA	intron variant	1	0
25	rs140291341	124462326	TGGAGTTTGT	G	A	TTCTTGCTAA	intron variant	1	0
25	rs535121	124462414	AAACTCTGCA	C	T	GCATTTACAG	intron variant	54	6
25	rs2289839	124462607	TTGGCAACAT	C	T	CAAGAGATCT	synonymous codon	16	0
25	rs139954729	124462620	AGAGATCTAC	G	A	ATTTCCATAA	missense	1	0
25	rs188800423	124462673	CACTTAGGCC	G	T	TAAAAACCAG	intron variant	1	0
25	rs78944687	124462707	CAAGAAGTGG	A	G	TCAAAGGCGA	intron variant	5	0

and alcohol and cocaine dependence. This known minor allele (rs139954729) is predicted by PolyPhen27 to be probably damaging, with a score of 0.981 (sensitivity: 0.75; specificity: 0.96). It was not found in European ancestry subjects in a large exome sequencing data set, NHLBI GO Exome Sequencing Project (ESP) (n=4300; http://evs.gs.washington.edu/EVS/). However, it is found in African American subjects (n=4404 chromosomes), but with a very low population frequency (0.044%). We could not establish the statistical evidence for the association with schizophrenia due to the limited sample size and incidence of the variant. Nevertheless, we sought to determine whether it would lead to cellular phenotypes, given that the variant was identified in a schizophrenia patient and his sibling with other neuropsychiatric disorders, as well as its low population frequency and the predicted deleterious property.

2.3: Biochemical characterization of the D1338N variant

The p.D1338 residue is located in the Rac1-GEF domain of *KALRN*, and charged amino acids are highly conserved across species and in related protein family members (Figure 2), so we hypothesized that a substitution that changes the charge from an acidic to a slightly basic residue in this domain is likely to affect protein function. To determine whether this would be the case, we transfected HEK 293 cells with a rat cDNA homologous to either the human major allele (referred to hereafter as "wildtype kalirin-7") or D1338N kalirin-7 constructs and performed a Rac1 activation affinity assay (Figure 3A). As expected, overexpression of wildtype kalirin-7 induced approximately a fourfold increase in Rac1-GTP levels compared to untransfected cells (Figure 3B). While overexpression of the D1338N variant led to an increase in Rac1 activation

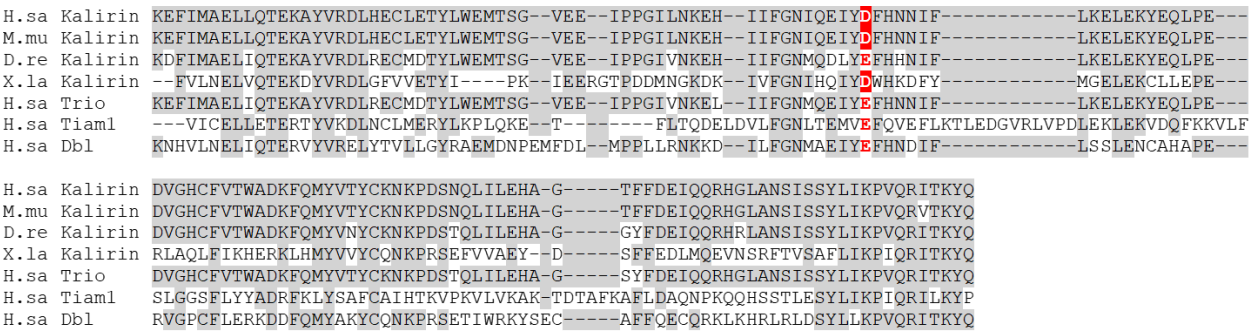

Figure 2. Alignment of the DH domains of several species' kalirin coding genes and human genes for kalirin-related GEFs. Note the conservation of the basic residues aspartic acid (white text on red background) and glutamic acid (red text on white background) at the homologous position of human kalirin amino acid 1338. H. sa, Homo sapiens; M. mu, Mus musculus; D. re, Danio rerio; X. la, Xenopus laevis.

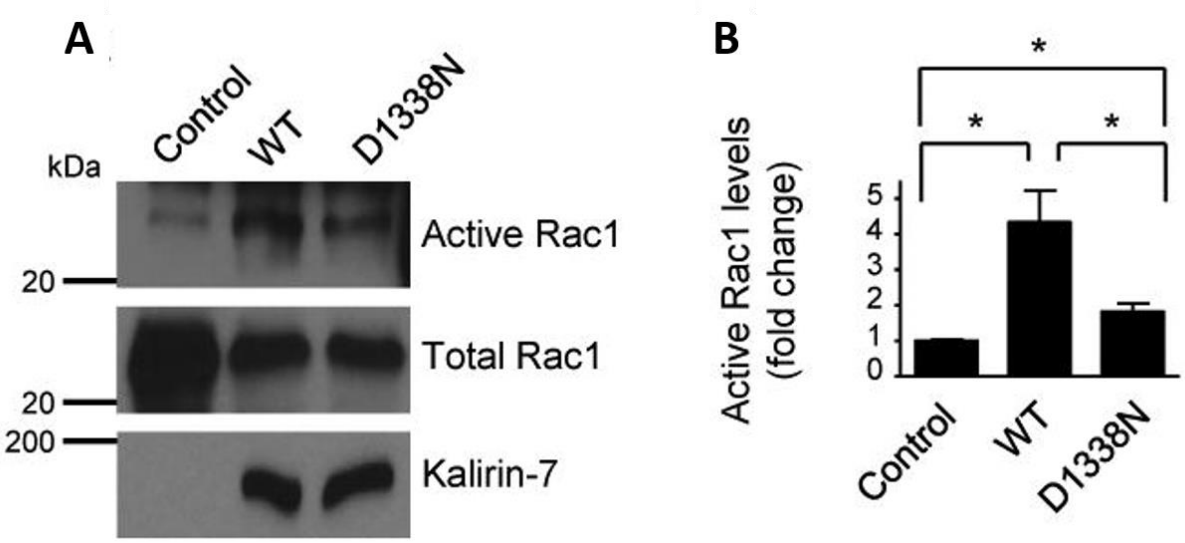

Figure 3. Biochemical consequences of the D1338N variant. (**A**) Activation of Rac1 is attenuated in HEK 293 cells expressing kalirin-7-D1338N as compared to those expressing wildtype (WT) kalirin-7. Rac1-GTP was isolated by incubation of cell lysates with a GST-PAK binding domain fusion protein, and levels were normalized to total Rac1 and kalirin-7 expression. (**B**) Quantification of Rac1 activation. Three independent experiments were performed, each of which involved transfection of two wells of cells per condition. *: $p < 0.05$. Data are mean ± SEM.

as compared to the untransfected condition, the degree of activation was significantly less than that induced by wildtype kalirin-7 (Figure 3B). These results indicate that the D1338N kalirin-7 variant is impaired with respect to the protein's ability to catalyze the exchange of GDP for GTP bound to Rac1 and may lead to alterations in cellular processes which are dependent on Rac1 signaling.

As many of the downstream effectors of Rac1 are known to cause remodeling of the actin cytoskeleton, we reasoned that a kalirin-7 variant that has impaired GEF activity would also be less able to stimulate actin polymerization. Rac1 overexpression in fibroblasts leads to a reorganization of actin filaments at the periphery of the cell, producing membrane ruffles and lamellipodia (A. Hall, 1998). We have previously shown that membrane ruffling, a morphological indicator of actin polymerization in 3T3 cells, can be induced by expression of either full length kalirin-7 protein or the kalirin-7 GEF domain alone (Penzes et al., 2000). Therefore, we examined the effect of the D1338N variant on membrane ruffling in COS-7 cells (Figure 4A). The majority of cells expressing wildtype kalirin-7 exhibited membrane ruffling along greater than 80% of their perimeters, representing a significantly greater degree of actin polymerization than that induced by kalirin-7-D1338N (Figure 4B). Thus, the kalirin-7-D1338N variant's diminished capacity for Rac1 activation has functional consequences in the context of cytoskeletal reorganization.

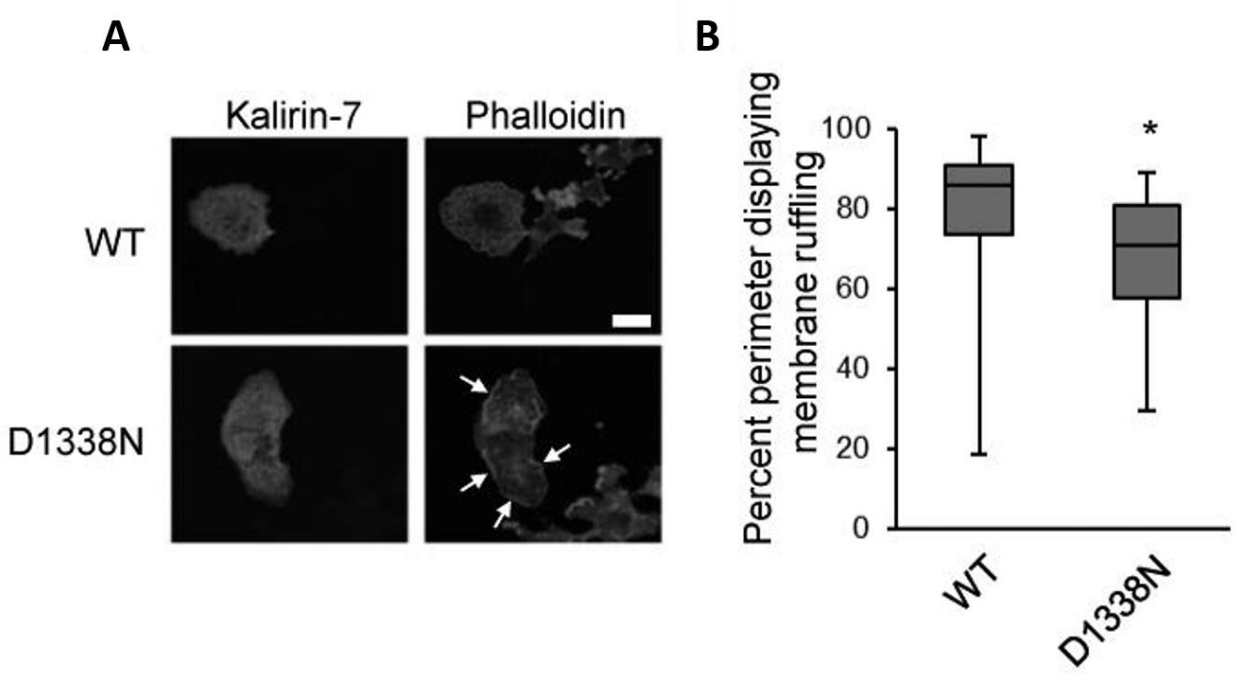

Figure 4. Actin polymerization in response to the D1338N variant. (**A**) COS-7 cells expressing myc-kalirin-7-D1338N (lower panels) exhibit a lesser degree of membrane ruffling, as visualized by staining with Alexa488-conjugated phalloidin, than do those expressing wildtype kalirin-7 (upper panels). The cell in the upper left panel displays ruffles on nearly 100% of its perimeter, whereas the cell in the lower left panel only displays ruffles in distinct locations (arrows). (**B**) Quantification of the degree of membrane ruffling in cells expressing either wildtype kalirin-7 or myc-kalirin-7-D1338N. Analysis of 30-35 cells was performed for each condition. *: $p < 0.05$. Data are mean ± SEM. Scale bar: 10 μm.

2.4: Neuronal morphology in kalirin-7-D1338N expressing neurons

The processes of dendritic spine maturation, excitatory synapse potentiation, and de novo spine formation are all dependent on remodeling of the actin cytoskeleton (Penzes & Cahill, 2012; Penzes & Rafalovich, 2012). The requirement of kalirin-7 in regulating these processes in forebrain pyramidal neurons has been well established (Penzes & Jones, 2008; Rabiner, Mains, & Eipper, 2005). Specifically, overexpression of kalirin-7 in primary cortical cultures causes an increase in both spine area and spine density, and the Rac1 GEF activity of kalirin-7 is required for these changes (Penzes et al., 2003; Xie et al., 2007). As such, we sought to determine whether the D1338N substitution would impair kalirin-7's ability to promote spine growth and development (Figure 5A). In mature cortical pyramidal neurons (21-28 DIV), overexpression of kalirin-7-D1338N failed to enhance spine density and area, whereas wildtype kalirin-7 overexpression increased both spine parameters as expected (Figure 5B). These data indicate that the D1338N variant not only impacts kalirin-7 protein function, but also has severe effects on spine structural plasticity.

2.5: MR imaging of D1338N carriers

Spine morphology is thought to contribute to brain neuropil volume, and post-mortem analyses and structural MR imaging studies of the brains of patients have provided evidence for reduced spine density and cortical thickness in the prefrontal and auditory association cortices in schizophrenia. To explore whether the subjects carrying the kalirin-7-D1338N variant displayed

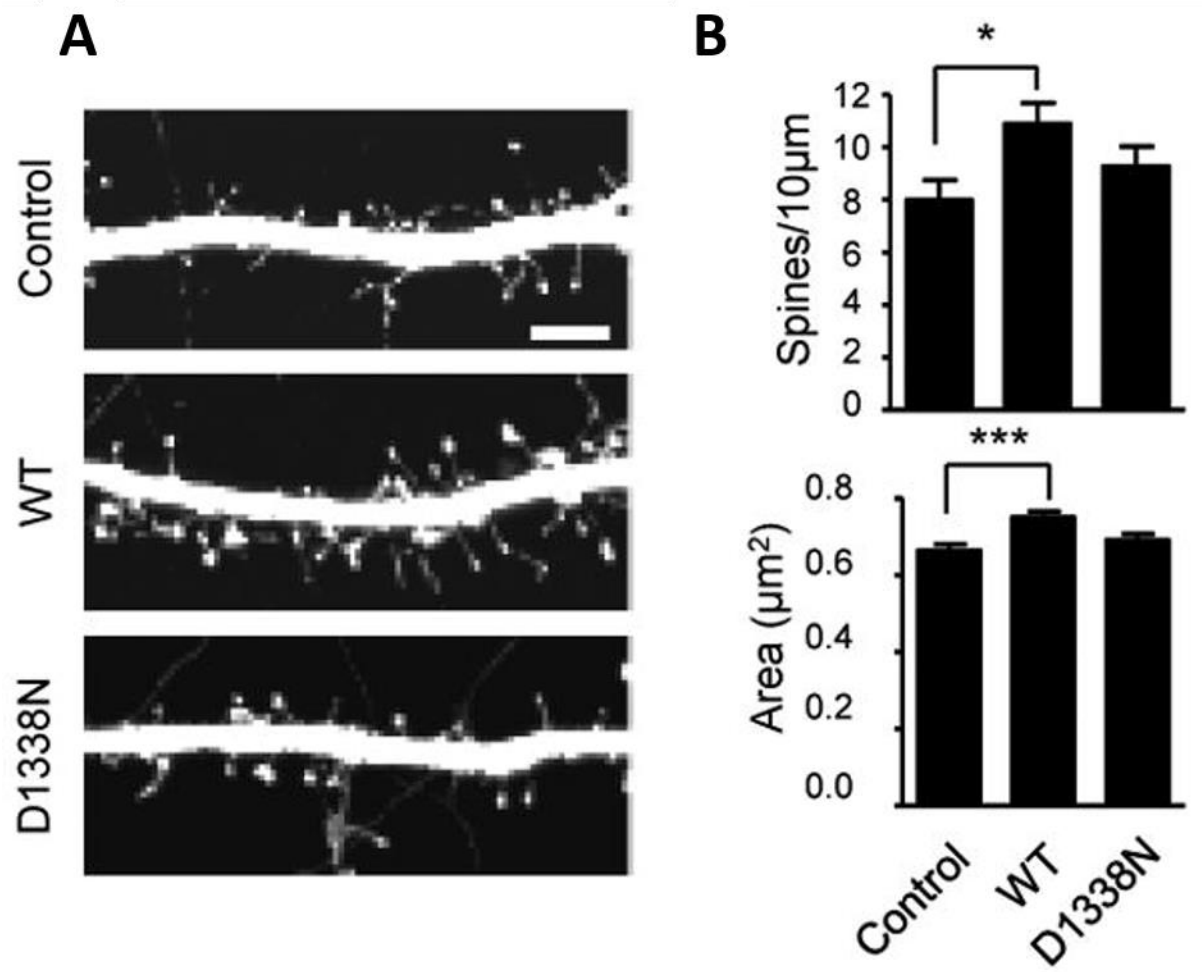

Figure 5. Dendritic spine density and area following kalirin-7 transfection. (**A**) Rat cortical pyramidal neurons were transfected with an eGFP expression vector alone (top panel), or with wildtype kalirin-7 (middle panel) or kalirin-7-D1338N (bottom panel). (**B**) Quantification of spine density (upper panel) and spine area (lower panel) reveals an increase in both parameters in the neurons overexpressing wildtype kalirin-7. No change was seen following overexpression of kalirin-7-D1338N. *: $p < 0.05$; ***: $p < 0.001$. Data are mean ± SEM. Scale bar: 5 µm.

unique neuromorphometric features, we compared MRI measures of cortical thickness between the carrier subjects and non-carriers. This preliminary comparison suggested that both the subject with schizophrenia (KAL-SCZ) and the sibling with depression (KAL-SIB) had reduced cortical thickness in the posterior banks of the left superior temporal sulcus (STS) as compared with the means of comparison groups of schizophrenia subjects (SCZ), their unaffected siblings (SCZ-SIB), and control subjects (CON) (Figure 6A, B).

2.6: Thinner cortex in Kalrn-*deficient mice*

Because a causal relationship between the D1338N variant and STS thickness cannot be established in this case due to lack of statistical power, we sought to determine whether reduced kalirin signaling in animal models could result in cortical morphological phenotypes consistent with the neuroimaging human phenotypes. We have previously reported that total knockout of the *Kalrn* gene in mice leads to reduced cortical thickness, as measured in the frontal cortex (Cahill et al., 2009; Xie et al., 2010). We therefore analyzed cortical neuropil area in the secondary auditory and temporal association cortices of *Kalrn* heterozygote mice, which better mimic the reduced kalirin signaling of the kalirin-7-D1338N variant in human subjects as compared to homozygous *Kalrn* knockout mice (Figure 7A). We labelled cell bodies by performing Nissl staining on coronal sections from 12-week-old mice, and defined neuropil as the area of the tissue that was devoid of stain. *Kalrn* heterozygotes exhibited a significant reduction in neuropil area as compared to wildtypes (Figure 7B) (92.4 ± 0.8% of wildtype area). These data indicate the necessity of intact functional kalirin expression for normal cortical morphology.

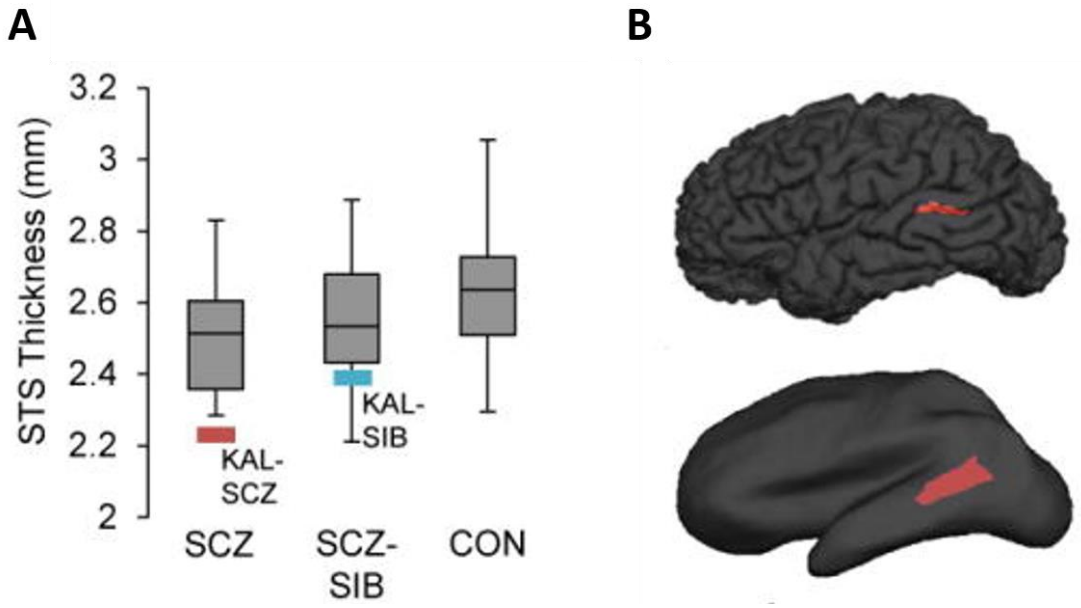

Figure 6. Impact of kalirin-7-D1338N on cortical thickness in human carriers. (**A**, **B**) Both KAL-SCZ (red bar) and KAL-SIB (blue bar) had reduced cortical thickness in the left superior temporal sulcus (STS; location on pial and inflated surfaces illustrated in the upper and lower panels, respectively, of (**B**)) as compared to the means of their respective experimental groups. The STS thickness measurement for KAL-SCZ was 1.72 standard deviations lower than the SCZ group mean.

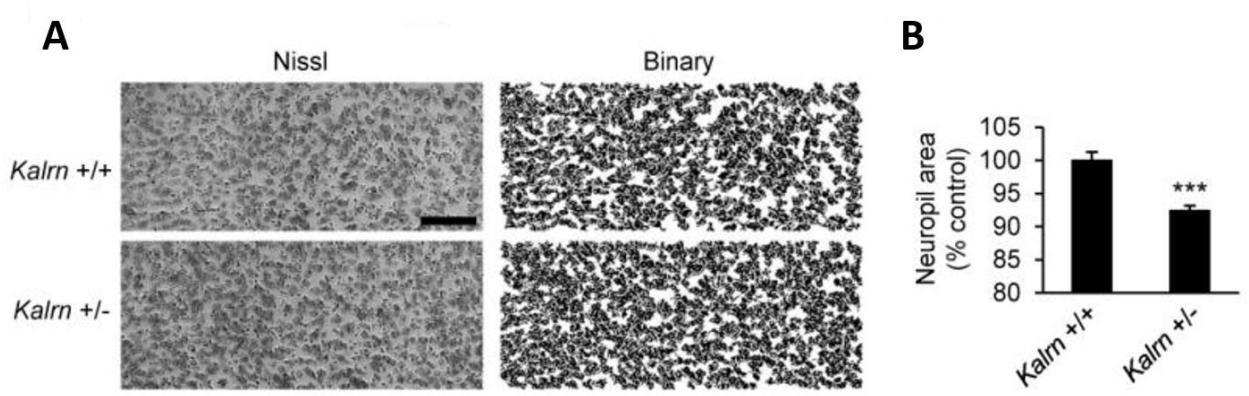

Figure 7. Impact of kalirin-7 hypofunction on cortical thickness in mice. (**A**) Analysis of neuropil area in the temporal association cortex of 12-week-old wildtype mice (upper panels) and litter-matched heterozygous *Kalrn*-null mice (lower panels) revealed a reduction in neuropil in mice carrying only one functional *Kalrn* allele. Neuropil was calculated by performing Nissl staining (left panels), binarizing and filtering images of the tissue (right panels), and calculating the area of the images not occupied by neuronal somata. (**B**) Quantification of neuropil area. Eight to twelve images were acquired from each of three or four animals per genotype. ***: $p < 0.001$. Data are mean ± SEM. Scale bar: 100 μm.

2.7: Discussion

Recent genomic studies have revealed extensive interindividual variability and diversity in the human genome, including common and rare variants, missense and nonsense mutations, and copy number variants (Human Genome Structural Variation Working et al., 2007; Iafrate et al., 2004). Genome-wide association and copy number variation studies of schizophrenia and other psychiatric disorders have identified many new disease susceptibility genes involving both common single nucleotide polymorphisms (SNPs) and rare disease variants, most of which contribute small effects (Duan, Sanders, & Gejman, 2010). In addition, variations in a number of genes have been associated with mental disorders such as schizophrenia (Myers et al., 2011; Sebat et al., 2009). It has been suggested that variations that increase risk for mental disorders cluster in gene networks that controls the synapse development and plasticity (Glessner et al., 2010). However, few studies have examined sequence variation in human genes encoding synaptic proteins, their molecular and cellular functional consequences, and their potential impact on human brain neuroimaging and phenotypes.

In the current study, we have established the presence of a rare *KALRN* sequence variant in a patient-sibling pair, which results in a single amino acid change in the kalirin-7 protein's catalytic GEF domain. Although we did not establish this variant as a risk for schizophrenia, it is predicted to be deleterious and present at a very low frequency in the human population. Additionally, while the sibling carrying the variant did not present with schizophrenia, she had been diagnosed with major depressive disorder, the treatment of which has been linked to increased dendritic spine

formation (Li et al., 2010). Pleiotropy is commonly seen in psychiatric disorders and other complex traits (reviewed in (Duan et al., 2010)). A schizophrenia susceptibility locus may be associated with not only other psychiatric disorders (Cross-Disorder Group of the Psychiatric Genomics, 2013; Cross-Disorder Group of the Psychiatric Genomics et al., 2013), but also some other non-psychiatric disorders, such as multiple sclerosis (Andreassen et al., 2015) and cardiovascular-disease (Andreassen et al., 2013). Among psychiatric disorders, such shared genetic susceptibility may be due the shared subphenotypes. Symptoms of mood disorder are common among individuals with schizophrenia (Silveira & Seeman, 1995), and they are also observed in their relatives at rates higher than those observed in the general population. Additionally, in young adults, depression may be a prodromal sign of psychosis (Herz & Melville, 1980). Moreover, variations in clusters of genes, including *KALRN*, implicated in schizophrenia and psychotic bipolar disorder etiology may impact resting state functional activity in affected individuals and first-degree relatives. This attests to the impact of common and rare genetic variation on measurable functional outcomes potentially related to disease phenotypes (Meda et al., 2014). One hypothesis for the minor allelic variant in *KALRN* would be that this variant alters cortical thickness, a subphenotype that manifests as schizophrenia or major depressive disorder depending on other genetic modifiers or different individual genetic backgrounds.

We have previously demonstrated that *Kalrn* null mice have thinner frontal cortices decreased spine number and dendritic arborization as compared to wildtypes (Cahill et al., 2009; Xie et al., 2010), and we show here that they have thinner temporal association cortices. Interestingly, the human subjects carrying this variant have a thinner cortex in the STS. The STS is part of a network that includes the medial prefrontal cortex and amygdala and is involved in aspects of social

cognition, including empathy and theory of mind. Patients show abnormal activation of this network during tasks involving the rating of emotional valence in facial expression (Brunet-Gouet et al., 2011), and flat affect item score is negatively correlated with performance on these tasks (Gur et al., 2006). While the scope of our analyses is limited by statistical power and does not demonstrate a causal relationship between p.D1338N and specific endophenotypes in carriers, our published and current data on *Kalrn* knockout mice may fill in the gap to some extent. Mouse knockout data suggest a causal relationship between reduced kalirin function and the regulation of both neuropil size and cortical morphology (Cahill et al., 2009; Xie et al., 2010). Since such morphological alterations are reminiscent of the structural abnormalities seen in schizophrenic patients (Karlsgodt et al., 2008; Rapoport et al., 1999), the role of kalirin in regulating cortical thickness in humans and animal models should be explored further.

There are important caveats in this study. Neither causality nor an association between the p.D1338N variant and any particular phenotype are established in this particular case, due to only two identified carriers. A more definitive test of association would require a large population case-control sample. Nevertheless, our study is one of the first to demonstrate that rare putatively deleterious variants in *KALRN* can lead to phenotypic changes relevant to schizophrenia. Our results are significant in the context of known supporting evidence for the association of both common and rare variants in *KALRN* with schizophrenia. The most significant association of a common variant in *KALRN* in the Psychiatric Genomics Consortium schizophrenia GWAS data set had a p-value of 5×10^{-4} (Ripke et al., 2013). Although the associations of common *KALRN* variants with schizophrenia have not reached genome-wide significance, they have been observed in other previous GWAS using different ethnic samples (Ikeda et al., 2011; Sullivan et al., 2008).

Resequencing *KALRN* in a Japanese sample further suggested that rare (MAF < 0.01) putatively functional missense SNPs may also contribute to schizophrenia risk (Kushima et al., 2012). Finally, the preliminary, uncorrected STS finding should be treated with caution. The effect of *KALRN* on cortical thickness may be relatively weak therefore requiring more subjects for increased statistical power.

It should be noted that there have been no single rare coding SNPs that are identified to show a statistically significant association with schizophrenia, even in large exome sequencing projects (Fromer et al., 2014; Purcell et al., 2014). This does not exclude the possibility that some rare functional variants in certain genes do contribute to susceptibility, and intriguingly, rare coding variants are found to be enriched in synaptic genes (Fromer et al., 2014; Purcell et al., 2014). Our study focuses on the functionality of the *KALRN* gene and one of its variants, rather than association evidence. We have shown that relationships could in principle be drawn between rare genetic sequence variants and neuroimaging and diagnostic phenotypes, given the appropriate number of subjects. Knowledge about the cellular and circuit-level impact of rare genetic variants in human subjects may in future point to disease mechanisms: specific molecular domains or functions, such as enzymatic domains, protein-protein interaction motifs, or phosphorylation sites, affected by amino acid changes could provide clues to the downstream/upstream members of the pathway.

When done at a suitable scale, this approach may provide insight into the pathogenesis of mental disorders. The approach we have taken could be a blueprint for larger scale studies that combine

human genetics, cellular and molecular analysis of impact of mutations, and analysis of cognitive, behavioral, and neuromorphometric measures in carriers.

CHAPTER 3: A Schizophrenia-Linked *KALRN* Coding Variant Alters Neuron Morphology, Protein Function, and Transcript Stability

3.1: Background

Previously, a schizophrenia-associated nonsynonymous SNV in the human *KALRN* gene (rs143835330) that codes for a proline-to-threonine substitution was identified and subsequently confirmed in multiple cohorts (Kushima et al., 2012). The allele frequency of the P2255T variant was shown to be 0.011 in schizophrenia patients as compared with 0.005 in control subjects. This variant has an odds ratio (OR) of > 2, a higher effect size than any previously reported for other schizophrenia-associated nonsynonymous coding variants (Sullivan, Daly, & O'Donovan, 2012). Thus, this variant could conceivably cause changes in kalirin protein function that could in turn influence the development of schizophrenia symptoms.

Alternative splicing of *KALRN* gives rise to several protein isoforms, the major ones being kalirin-7, kalirin-9, and kalirin-12 (Penzes et al., 2001). Of these, the P2255 residue is only present in the longer kalirin-9 and kalirin-12 isoforms. These proteins include several protein-protein interaction domains, along with both Rac-GEF and Rho-GEF domains (Figure 8) (Johnson et al., 2000). In general, Rac1 promotes dendrite arborization and spine growth and stabilization, while RhoA inhibits these processes (Meng et al., 2002; Soderling et al., 2007; Wegner et al., 2008). Analysis of the network of kalirin-related gene products demonstrates a significant overlap between the kalirin network and genes that have been linked to schizophrenia via genome-wide association studies (Figure 9A, B) (Schizophrenia Working Group of the Psychiatric Genomics Consortium, 2014; Warde-Farley et al., 2010). These observations suggest that kalirin is involved in a network of synaptic proteins that are crucial for synaptic function, and whose disruptions likely contribute to schizophrenia pathology.

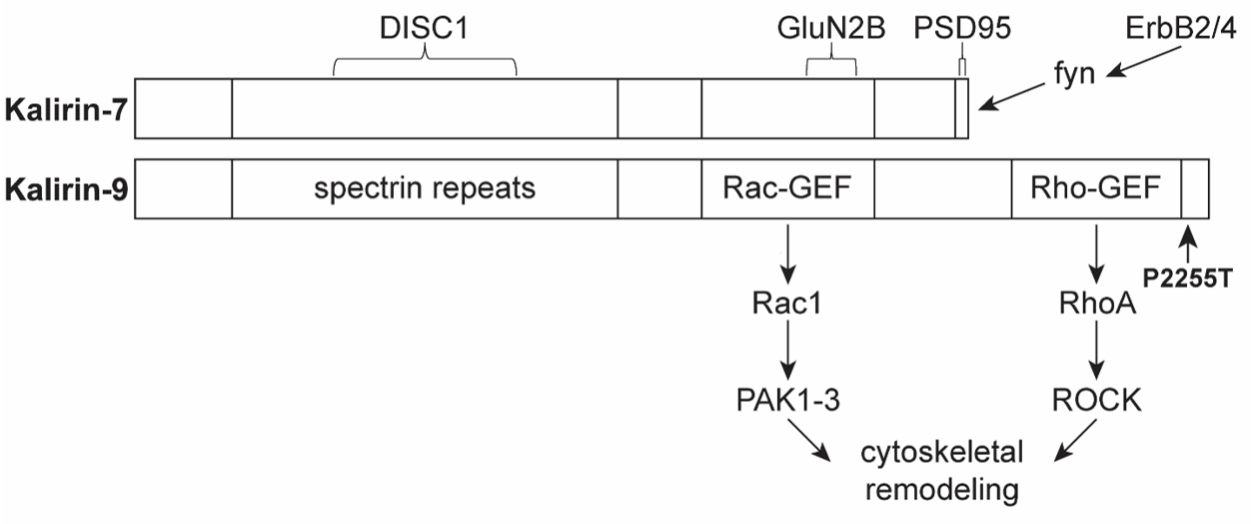

Figure 8. Schematic of the kalirin (Kal)-7 and Kal9 proteins. Catalytic domains, structural motifs, and upstream and downstream signaling pathways are illustrated. The location of the P2255T substitution is shown. DISC1, disrupted in schizophrenia 1; GEF, guanine nucleotide exchange factor; PAK, p21-activated kinase; Rac1, Ras-related C3 botulinum toxin substrate 1; RhoA, Ras homologue gene family, member A; ROCK, Rho-associated protein kinase.

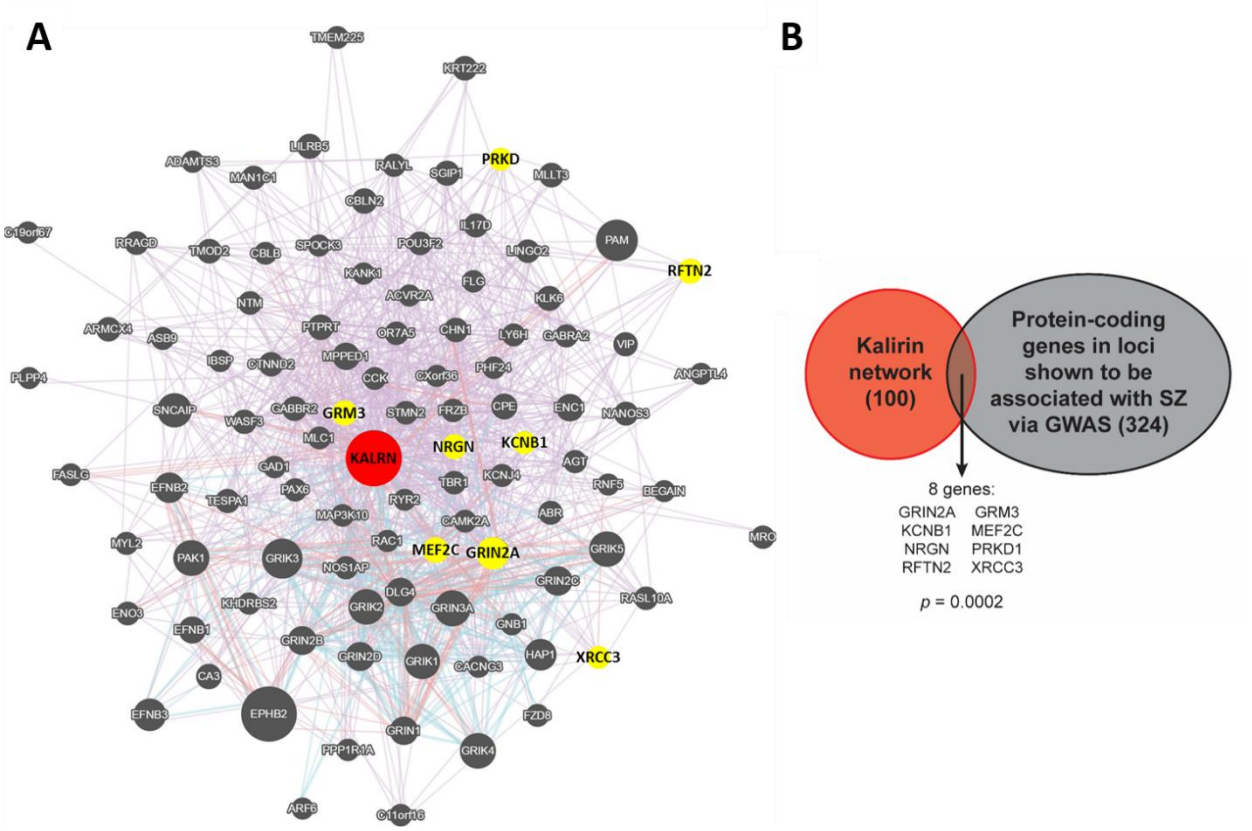

Figure 9. *KALRN* associations with schizophrenia (SZ). (**A**) Hypothetical *KALRN* interaction network, predicted based on co-expression, pathway, and physical interaction, and weighted with regard to cellular component gene ontology. Genes shown in yellow are also among those residing in SZ-associated loci identified by a large-scale genome-wide association study (GWAS). (**B**) Hypergeometric testing reveals a significant overlap between those genes in the hypothetical *KALRN* network and those identified by GWASs.

Therefore, we investigated the role of the P2255T variant expressed in the kalirin-9 isoform background. Structured illumination microscopy revealed differential subsynaptic distribution of kalirin isoforms. We found that overexpression of the P2255T variant led to morphological changes in cultured neurons that are consistent with those seen in schizophrenia. Additionally, we also observed increased mRNA stability of kalirin-9-P2255T, leading to increased mRNA expression and protein levels compared with control subjects. Finally, we determined that the P2255T increased kalirin-9 Rho-GEF activity but had no effect on Rac-GEF activity. Thus, the combination of both altered protein function and increased protein levels likely contributes to the pathogenesis of schizophrenia in patients carrying this SNV. This mutation provides an effective model for further investigating convergent pathways underlying perturbed dendritic morphogenesis in schizophrenia.

3.2: Superresolution imaging reveals differential subsynaptic localization of kalirin isoforms

To establish the subcellular sites where kalirin-9-P2255T–dependent cellular phenotypes may be more evident, we examined the relative subcellular distribution of major kalirin isoforms. Previous studies have shown distinct patterns of localization of endogenous kalirin isoforms in cultured neurons, with kalirin-7 being observed in puncta along the dendrites, kalirin-9 being expressed throughout the dendrites, and kalirin-12 being predominantly expressed in the soma (Johnson et al., 2000). However, these studies were performed in young (2-7 DIV) neurons, and no such studies have been performed in mature neurons. To determine the relative spatial localization of kalirin isoforms in mature neurons, we used structured illumination microscopy, a superresolution

method (Gustafsson, 2005) to determine the precise localization of kalirin-7 and kalirin-9 (Figure 10A). Notably, the relative subsynaptic distribution of different isoforms of a postsynaptic protein has not yet been examined at the subdiffraction level. Whereas kalirin-7 was present in 75% of spines, kalirin-9 was spredominantly expressed in shafts or excluded entirely, with only 31% of spines that were examined expressing this isoform (Figure 10B). Furthermore, although spines that included kalirin-7 tended to be significantly larger than those that did not, the presence of kalirin-9 in spines did not correlate with spine morphology (Figure 10C). These data suggest that spatial patterning of kalirin isoforms may play an important role in dendrite and spine structure, with kalirin-9 likely exerting its primary effects on cytoskeletal remodeling in dendrites.

3.3: Kalirin-9-P2255T reduces basal dendrite branching

Several groups have found abnormalities in dendritic arborization in the cortices and hippocampi of schizophrenia patients (Benes & Berretta, 2001; Broadbelt et al., 2002; Cotter, Wilson, Roberts, Kerwin, & Everall, 2000; Kalus et al., 2000; Rosoklija et al., 2000). To determine the impact of the P2255T SNV on dendritic morphology, we overexpressed wild-type kalirin-9 (kalirin-9-WT) or kalirin-9-P2255T along with green fluorescent protein (GFP), or GFP alone, in cultured cortical neurons (25-26 DIV) (Figure 11A). As expected based on previous studies (Deo et al., 2012), overexpression of kalirin-9-WT led to significant reductions in both basal and apical dendritic complexity as compared with cells transfected with only GFP (Figure 11B). Kalirin-9-P2255T overexpression led to a significant reduction of proximal dendritic complexity as compared with kalirin-9-WT (Figure 11B, left panel). This overall reduction was due to an approximate 25% reduction in the number of basal dendrites

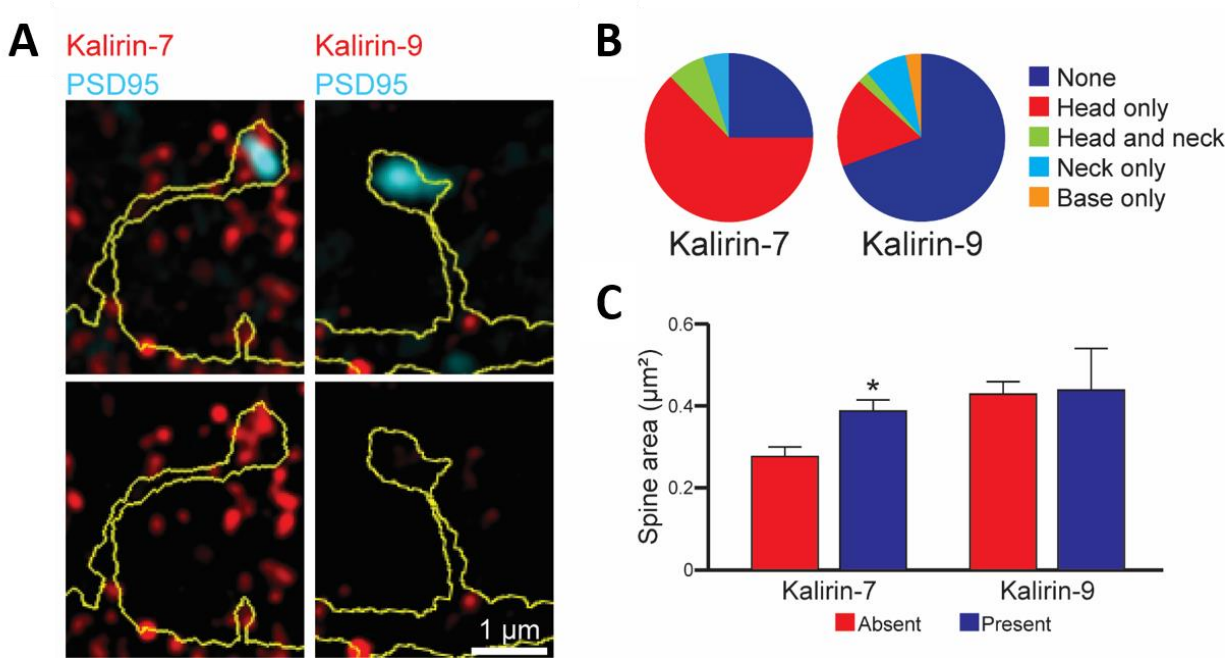

Figure 10. *KALRN* expression in mature neurons. (**A**) Structured illumination microscopy imaging of mature (days in vitro 25–26) cortical neurons demonstrates that endogenous Kal7 is localized in the majority of postsynaptic density protein 95 (PSD95)–containing spines, whereas Kal9 is largely excluded from spines. (**B**) Proportions of spines with Kal7 and Kal9 expression in distinct nanodomains. Blue indicates no expression; red indicates head only; green indicates head and neck; light blue indicates neck only; orange indicates base only. (**C**) Spines lacking Kal7 are significantly smaller than those with Kal7 (n = 98 spines). The presence of Kal9 in a spine has no bearing on its size (n = 113 spines). Cells from three independent experiments were analyzed. Data are mean ± SEM. *p < .05.

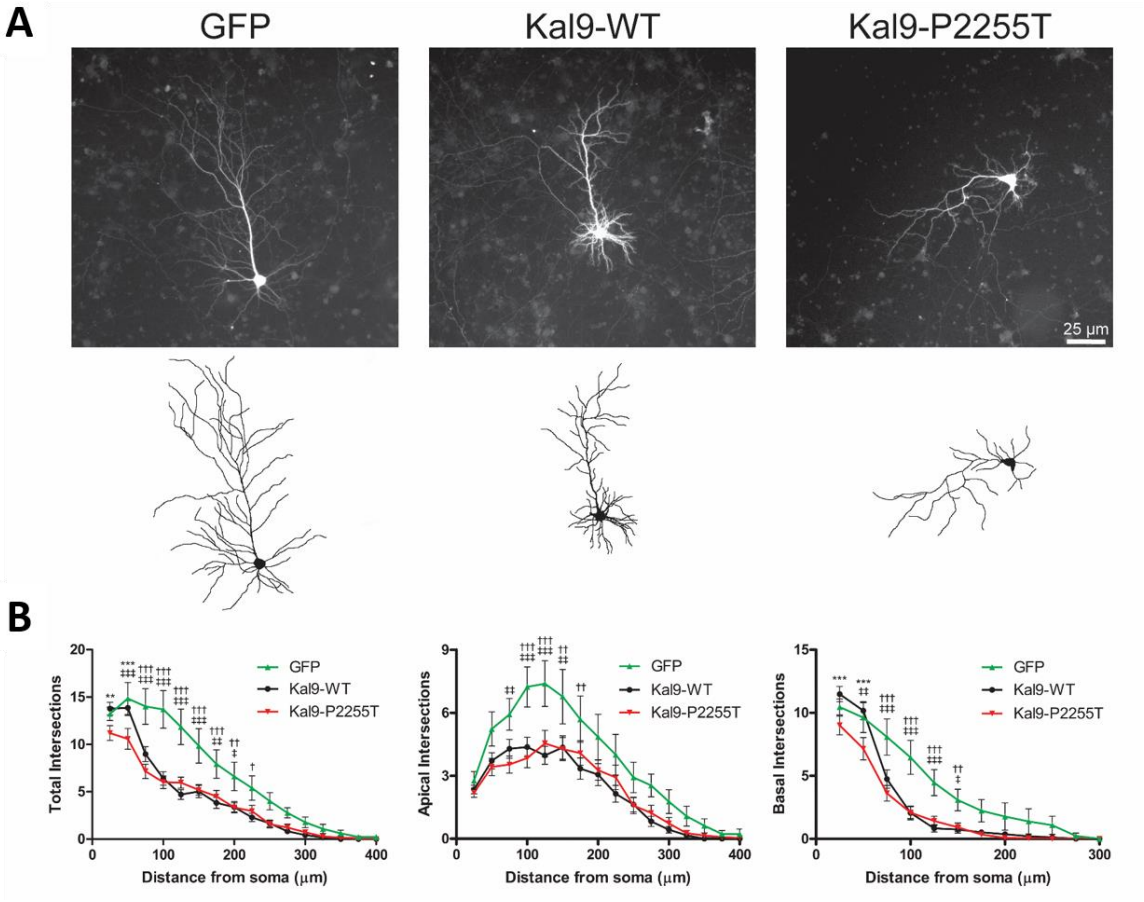

Figure 11. Kal9-P2255T diminishes basal dendrite branching in cortical pyramidal neurons. (**A**) Days in vitro 25–26 neurons transfected with either green fluorescent protein (GFP) alone, or with GFP and either Kal9-WT or Kal9-P2255T (upper panels); and traces used for Sholl analysis (lower panels). (**B**) Sholl analysis reveals a significant reduction in basal dendrites of neurons expressing Kal9-P2255T extending 25 and 50 µm from the soma as compared with Kal9-WT. Apical dendrites were unchanged. n = 20–35 neurons per transfection condition from three independent experiments. Data are mean ± SEM. **: $p < .01$, ***: $p < .005$ (Kal9-WT vs. Kal9-P2255T). †: $p < .05$, ††: $p < .01$, †††: $p < .005$ (Kal9-WT vs. GFP). ‡: $p < .05$, ‡‡: $p < .01$, ‡‡‡: $p < .005$ (Kal9-P2255T vs. GFP).

extending 25 and 50 μm from the soma (Figure 11B, right panel). The functional consequences of this reduction are unknown; however, the synapses on proximal versus distal basal dendrites are known to undergo distinct mechanisms of plasticity and have distinct roles in the temporal and spatial summation of excitatory inputs (Branco & Hausser, 2011; Gordon, Polsky, & Schiller, 2006).

3.4: Kalirin-9-P2255T diminishes dendritic spine head dimensions

Decreased dendritic spine density on cortical pyramidal neurons is one of the most consistently reported cytological abnormalities in schizophrenia, and patients have also been shown to display altered levels of several regulators of the actin cytoskeleton in spines (Yan, Kim, Datta, Lewis, & Soderling, 2016). Although kalirin-9 is not expressed at high levels in spines themselves, its activation of Rho family GTPases may lead to the diffusion of these signaling molecules into spines, where they may exert effects on spine morphology. Therefore, we assessed the density and dimensions of spines in neurons overexpressing kalirin-9-WT as compared with kalirin-9-P2255T (Figure 12A). As shown before (Deo et al., 2012), kalirin-9-WT significantly increased spine breadth, and also increased spine area, as compared with GFP. Kalirin-9-P2255T reversed this effect, as both spine area and breadth were significantly decreased in neurons transfected with kalirin-9-P2255T as compared with kalirin-9-WT, but were not significantly different from GFP alone (Figure 12B).

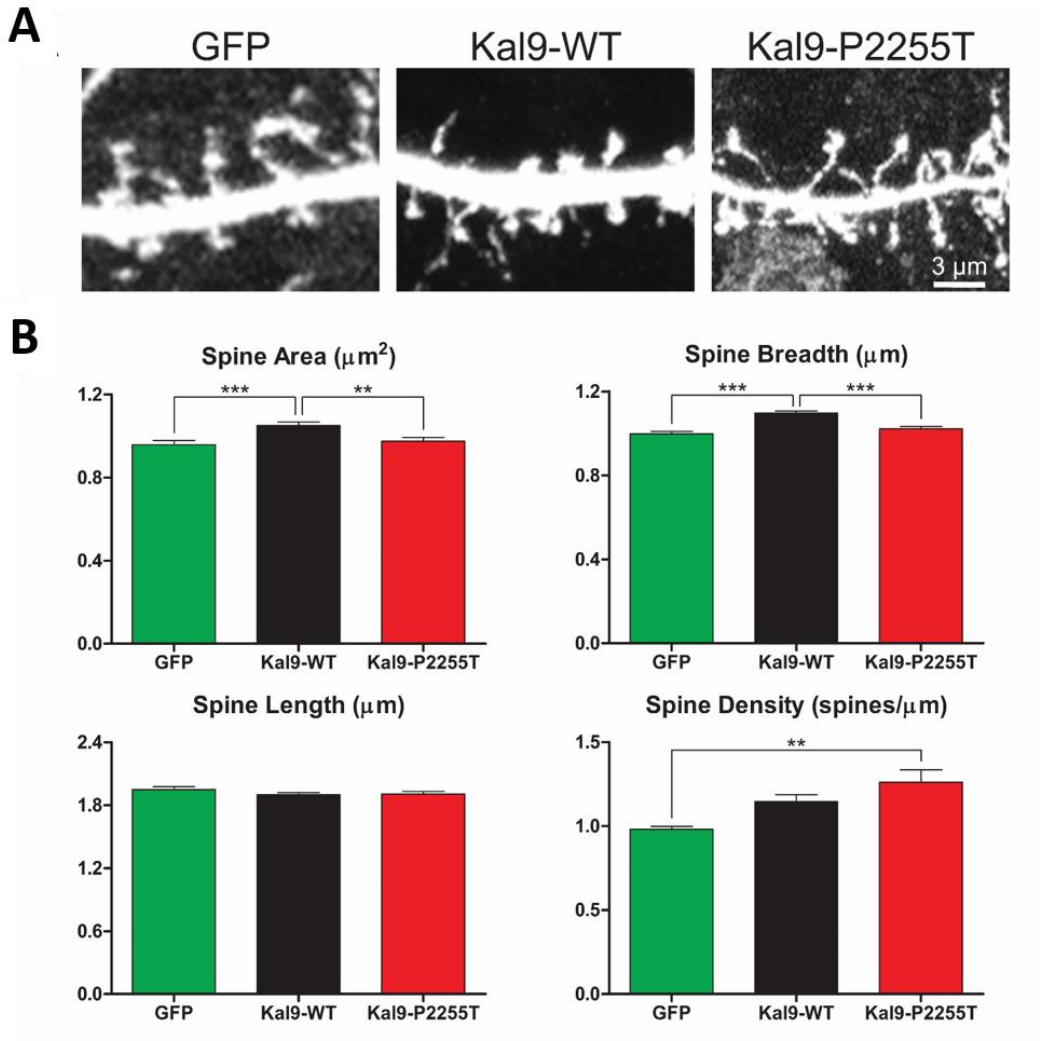

Figure 12. Kal9-P2255T fails to induce the increases in dendritic spine dimensions seen following Kal9-WT overexpression. (**A**) Days in vetro 25–26 cortical pyramidal neurons transfected with either green fluorescent protein (GFP) alone, or with GFP and either Kal9-WT or Kal9-P2255T. (**B**) Area and breadth of dendritic spine heads are significantly reduced in neurons expressing Kal9-P2255T as compared with Kal9-WT. Spine length and density were unaffected. n = 11–18 neurons per transfection condition from three independent experiments were analyzed. Data are mean ± SEM. **: $p < .01$, ***: $p < .005$.

3.5: Kalirin-9-P2255T protein is expressed at higher levels than kalirin-9-WT protein levels in neurons

Elevated levels of kalirin-9 were seen within the auditory cortex of individuals with schizophrenia as compared with psychiatrically normal control subjects (Deo et al., 2012), suggesting a potential role in pathogenesis. We therefore tested the impact of the P2255T SNV on kalirin-9 protein levels in cultured cortical neurons. We co-transfected cells at 14 DIV with GFP and either kalirin-9-WT or kalirin-9-P2255T, and allowed them to express the exogenous proteins for 72 hours. To exclude endogenous kalirin-9 we labeled the exogenous protein with a c-Myc antibody that only recognizes the exogenous tagged kalirin-9 (Figure 13A). After 72 hours, neurons showed a greater amount of kalirin-9-P2255T compared with kalirin-9-WT under identical transfection conditions (Figure 13B). To see if this increase in kalirin-9-P2255T protein was sustained, we allowed neurons to express exogenous proteins for 14 days. We found a similar trend to that seen for 72 hours, demonstrating that the increase in kalirin-9-P2255T is indeed sustained (Figure 13C). Normalization to GFP expression confirmed that the increase in the P2255T at 72 hours was not due to differences in transfection efficiency (Figure 13D). This recapitulation of the increased kalirin-9 expression in schizophrenia may therefore underlie the morphological changes seen in neurons expressing kalirin-9-P2255T.

3.6: Increased kalirin-9-P2255T protein is due to altered mRNA stability

To directly test the abundance and biological stability of kalirin-9-P2255T versus kalirin-9-WT, we transiently transfected kalirin-9-WT or kalirin-9-P2255T-expressing plasmids into HEK 293

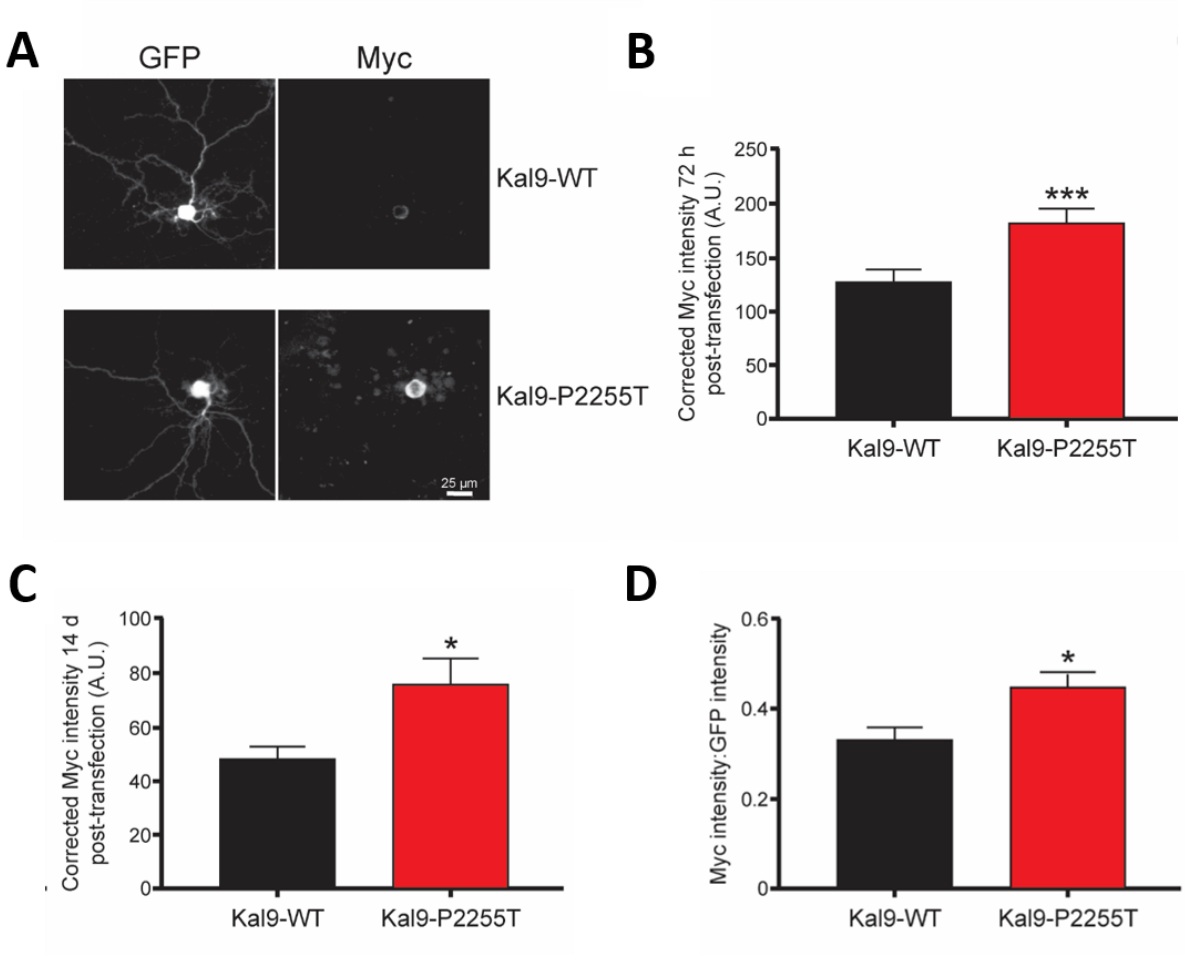

Figure 13. Kal9-P2255T protein is expressed more highly than Kal9-WT in neurons. (**A**) Days in vitro 28 cortical pyramidal neurons transfected with green fluorescent protein (GFP) and either Kal9-WT or Kal9-P2255T and stained for GFP and c-Myc. (**B**, **C**) Fluorescence intensity of Kal9-P2255T is greater than that of Kal9-WT at both (**B**) 72 hours and (**C**) 14 days post-transfection. (**D**) The ratio of c-Myc to GFP intensity reveals that the difference in expression at 72 hours is not due to a difference in transfection efficiency. n = 68–131 neurons per transfection condition from three independent experiments. All data are mean ± SEM. *: $p < .05$, ***: $p < .005$. A.U., arbitrary unit.

cells, along with GFP to assess for transfection efficiency. Quantitative reverse transcriptase polymerase chain reaction revealed that kalirin-9-P2255T mRNA levels were elevated compared with kalirin-9-WT under the same transfection conditions (Figure 14A). To test the relative stability of kalirin-9-WT versus kalirin-9-P2255T mRNA, after 24 hours of overexpression we used actinomycin D to inhibit RNA polymerase and thus any subsequent generation of new transcripts. The half-life curves generated for each transcript show that the single nucleotide difference in the kalirin-9-P2255T transcript leads to significantly more stable kalirin-9 mRNA (Figure 14B).

Stability of a specific mRNA molecule is partly determined by its secondary structure. To determine the impact of the P2255T SNV on the kalirin-9 mRNA (accession AF232668) secondary structure, we used the mfold software (version 3.6) with default parameters to generate an in silico prediction based on free energy minimization using parameters set forth by the nearest-neighbor model (Zuker, 2003). The kalirin-9-P2255T SNV was predicted to diminish the presence of an interior loop structure within a helix (Figure 14C). It should be noted, however, that predicted secondary structure changes may or may not carry over into alterations in biological stability, which is regulated by a combination of sequence-specific RNA-binding proteins, microRNAs, as well as by RNA secondary structure (Chamary & Hurst, 2005; Duan et al., 2003; Lennox, Mao, & Silver, 2017).

We next sought to determine if the kalirin-9-P2255T SNV also alters protein stability in HEK 293 cells transiently expressing kalirin-9-WT or kalirin-9-P2255T, along with GFP to normalize for transfection efficiency. Similar to what was seen in neurons, kalirin-9-P2255T protein levels were

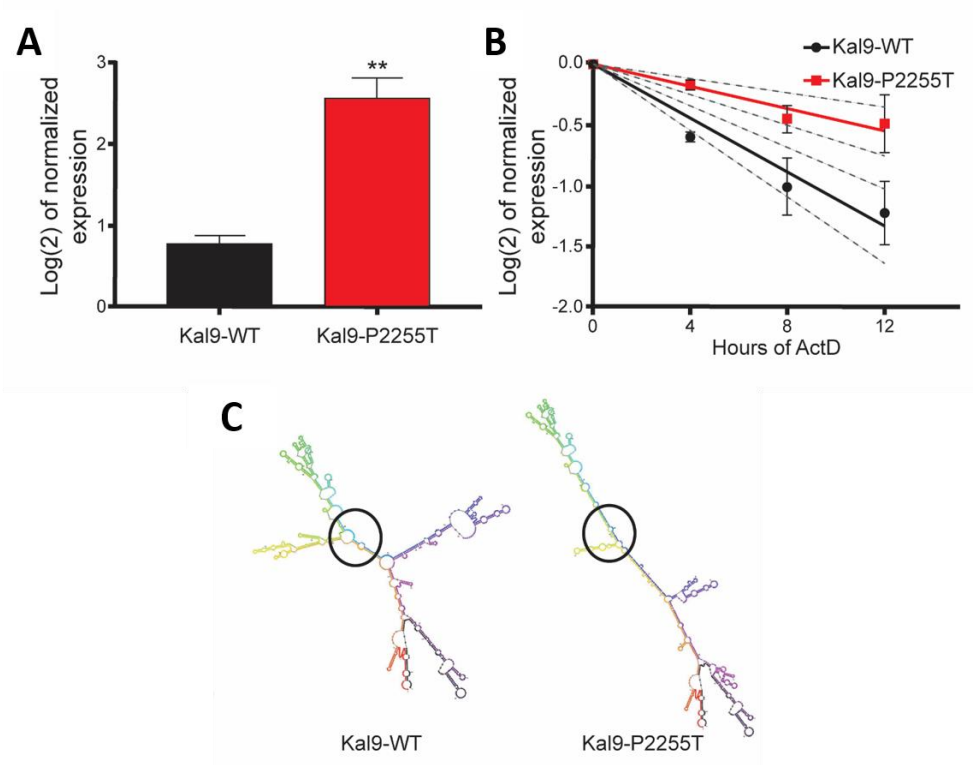

Figure 14. Kal9-P2255T messenger RNA is expressed more highly and is more stable than Kal9-WT in heterologous cells. (**A**) Isolated RNA from HEK 293 cells transfected with either Kal9-WT or Kal9-P2255T were subjected to qRT-PCR. Following normalization to β-actin expression, Kal9-P2255T messenger RNA levels are shown to be increased compared with Kal9-WT. Data are from four independent experiments. (**B**) Kal9-WT and Kal9-P2255T transfected HEK 293 cells treated with actinomycin D (ActD) for 4, 8, or 12 hours show differential rates of Kal9 transcript degradation. Half-life was calculated as ln(2)/-slope. t1/2 = 6.2 hours for Kal9-WT and 15.3 hours for Kal9-P2255T. Dashed lines represent 95% confidence intervals. Data are from three independent experiments. (**C**) mfold software predicts the disruption of an interior loop in the secondary structure of Kal9-P2255T messenger RNA. The nucleotide coding for amino acid 2255 resides in within the circles overlaying the images. All data are mean ± SEM. **: $p < .01$.

higher than kalirin-9-WT after 48 hours (Figure 15A, B). We then used cycloheximide to inhibit new protein synthesis and tested the comparative stability of residual kalirin-9-WT or kalirin-9-P2255T proteins. We allowed cells to express exogenous proteins for 24 hours, after which we treated cells with cycloheximide and examined kalirin-9 protein levels at three subsequent time points. The rate of protein degradation did not significantly differ between kalirin-9-WT and kalirin-9-P2255T (Figure 15C), indicating that the P2255T SNV does not change the stability of kalirin-9 protein.

3.7: P2255T substitution increases kalirin-9 RhoA-GEF catalytic activity

The P2255T substitution, while not in the Rho-GEF catalytic domain, occurs only 14 amino acids downstream of it, suggesting that it may affect this activity (Figure 8, arrow). Upregulation of RhoA activation by overexpression of another RhoA-GEF, ARHGEF11, or constitutively active RhoA, as well as the knockdown of the Rho GTPase–activating protein oligophrenin-1, has been shown to reduce dendritic complexity, spine area, and spine density (Govek et al., 2004; Mizuki et al., 2016; Nakayama, Harms, & Luo, 2000). We thus sought to determine whether kalirin-9-P2255T could elicit its effects on neuronal morphology through altered GEF activity. We expressed kalirin-9-WT and kalirin-9-P2255T in HEK293 cells and performed a RhoA activation affinity assay to evaluate their impact on GTP-bound RhoA (Figure 16A). To assess intrinsic activity independent on protein levels, we normalized to both total RhoA and exogenous kalirin-9 levels. kalirin-9-P2255T expression led to a significant increase in RhoA activation (Figure 16B). On the contrary, a similar assay used to measure Rac1 activation did not show any differences in Rac1 activation between kalirin-9-WT and kalirin-9-P2255T (Figure 17A, B).

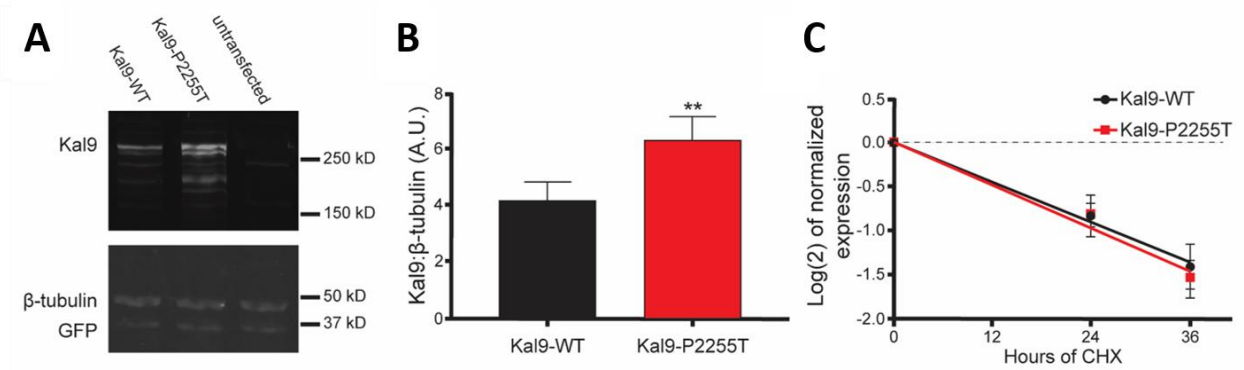

Figure 15. Kal9-P2255T protein is expressed more highly than Kal9-WT in heterologous cells. (**A**) Western blots of lysates from HEK 293 cells transfected with GFP alone, or GFP and either Kal9-WT or Kal9-P2255T. (**B**) When normalized to β-tubulin, Kal9-P2255T is shown to be expressed more highly than Kal9-WT. (**C**) Cycloheximide (CHX) treatment of transfected HEK 293 cells demonstrates that there is no change in the stability of Kal9-P2255T vs. Kal9-WT protein (see Supplemental Figure S2 for blot images). Data are from three independent experiments. All data are mean ± SEM. **: $p < .01$. A.U., arbitrary unit.

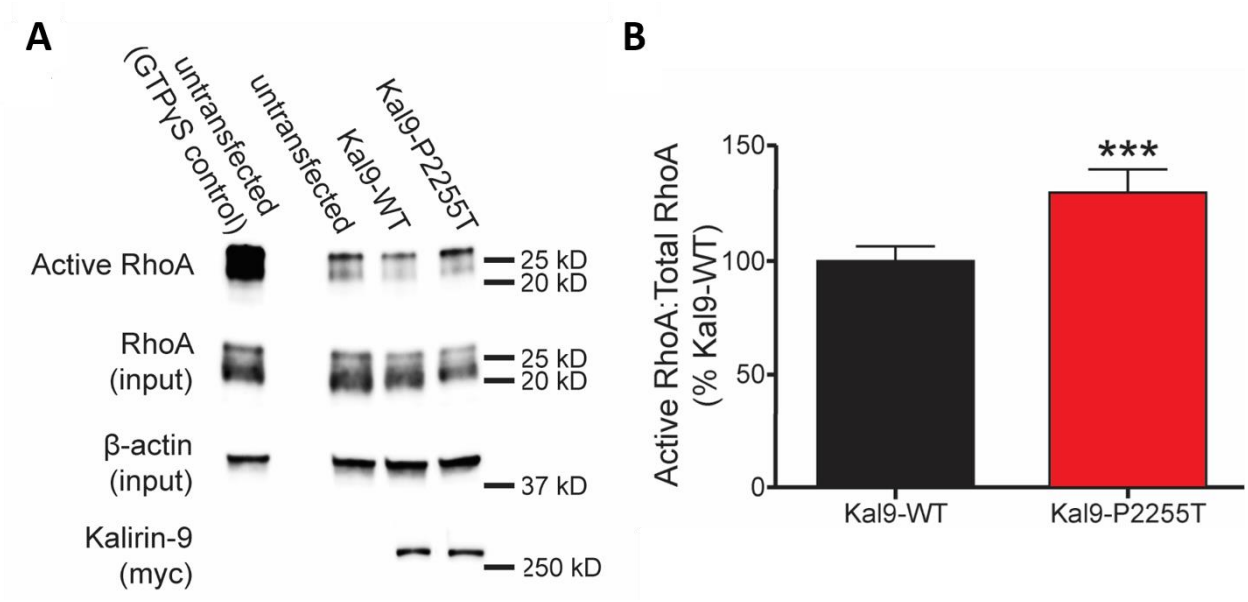

Figure 16. The P2255T substitution increases Kal9 RhoA-GEF catalytic activity. (**A**) Following transfection of HEK 293 cells with amounts of plasmid to account for altered Kal9 protein levels, Western blotting reveals that Kal9-P2255T–transfected cells display higher levels of guanosine triphosphate–bound RhoA than Kal9-WT–transfected cells. (**B**) Quantification of the blots in panel (**A**) Blots were normalized to total RhoA and β-actin levels. Data are from four independent experiments. All data are mean ± SEM. ***: $p < .005$. GTPγS, guanosine 5′-O-[gamma-thio]triphosphate.

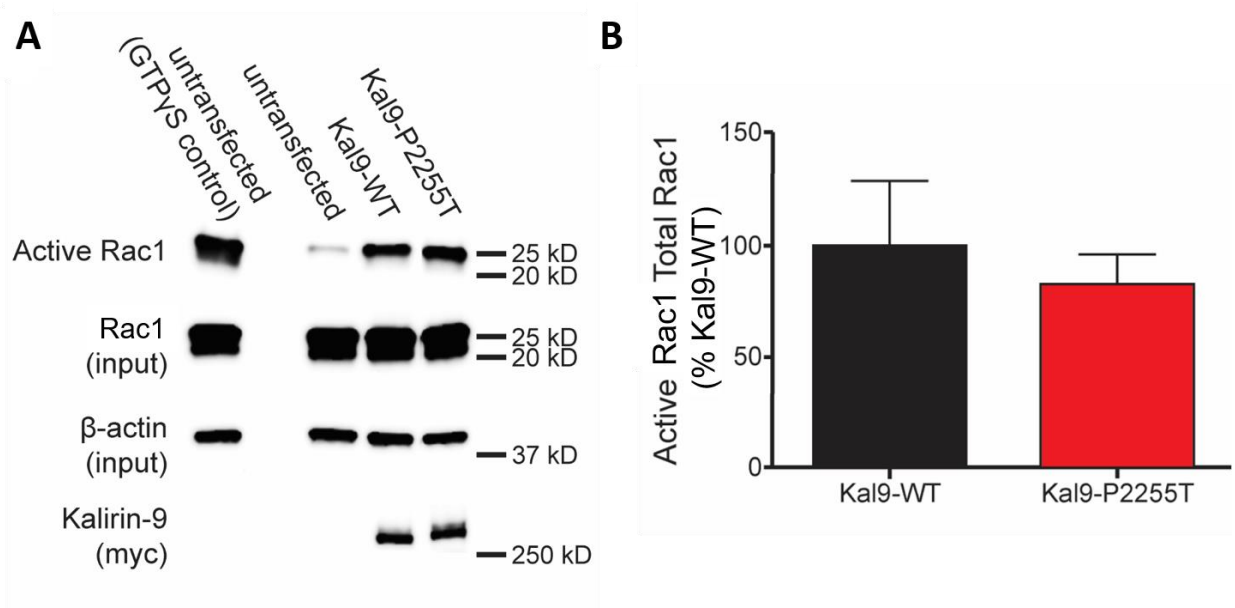

Figure 17. The P2255T substitution has no effect on Kal9 Rac1-GEF catalytic activity. (**A**) Under the same transfection conditions as in Figure 16, guanosine triphosphate–bound Rac1 levels show no difference between the Kal9-WT and Kal9-P2255T levels. (**B**) Quantification of the blots in panel (**A**) Blots were normalized to total Rac1 and β-actin levels. Data are from five independent experiments. All data are mean ± SEM. GTPγS, guanosine 5′-O-[gamma-thio]triphosphate.

3.8: Compound effect of mRNA stability and Rho-GEF activity in kalirin-9-P2255T

Because the signaling output of a protein is dependent on both intrinsic enzymatic activity and protein levels, we accounted for the differential protein levels between the WT and P2255T variants. We transfected equal amounts of kalirin-9-WT and kalirin-9-P2255T complementary DNA, and when performing RhoA activation assay we normalized to total RhoA (Figure 18A). We found that the RhoA-GEF activity of kalirin-9-P2255T was enhanced to an even greater degree as compared with kalirin-9-WT (Figure 18B). Thus, the compound effects of increased RhoA-GEF activity in kalirin-9-P2255T, with heightened levels carrying this variant, result in a significantly altered signaling output of the protein.

3.9: Discussion

Recent discoveries have found that exonic point mutations (SNVs) play an important role in the etiology of mental disorders, including schizophrenia (Fromer et al., 2014; Iossifov et al., 2014; Purcell et al., 2014). Exome sequencing of large numbers of schizophrenia patients and control subjects has revealed that small mutations, affecting only a few nucleotides, are overrepresented among glutamatergic postsynaptic proteins, including activity-regulated cytoskeleton-associated proteins, N-methyl-D-aspartate receptor complexes, and proteins that interact with these complexes to modulate synaptic strength (Fromer et al., 2014; Purcell et al., 2014). Such mutations are very rare (frequency < 0.5%). None of these SNVs individually was statistically associated with schizophrenia. However, the functional significance of such mutations, especially at sites relevant for these disorders such as dendrites and

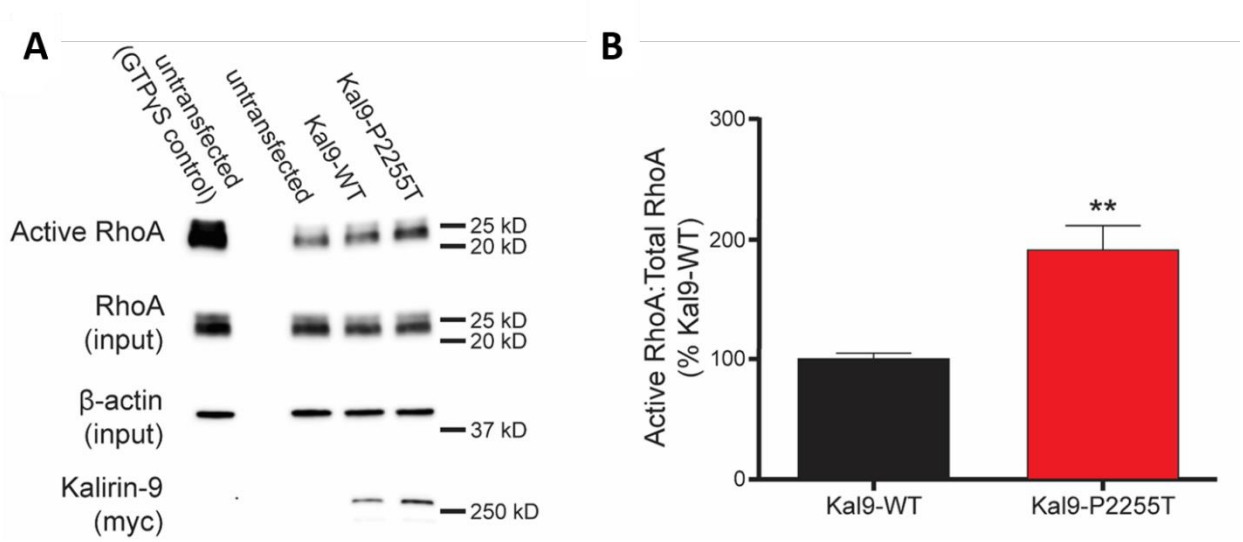

Figure 18. Combined effect of the increased protein expression and catalytic activity of Kal9-P2255T on RhoA activation. (**A**) When equal amounts of Kal9-WT and Kal9-P2255T plasmids are used for transfection, an even greater level of RhoA activation is seen in the Kal9-P2255T condition than that in the experiments described in Figure 16. (**B**) Quantification of the blots in panel (**A**) Blots were normalized to total RhoA and β-actin levels. Data are from three independent experiments. All data are mean ± SEM. **p < .01. GTPγS, guanosine 5′-O-[gamma-thio]triphosphate.

synapses, has not yet been examined. For these reasons we investigated the impact of a SNV in *KALRN*, enriched in subjects with schizophrenia, on the structure and function of dendrites and synapses in neurons. There currently exist few studies linking rare schizophrenia-associated SNVs to functional deficits. For example, several SNVs in the *GIT1* gene that were originally identified via exome sequencing of schizophrenia patients were demonstrated to perturb G protein–coupled receptor kinase interacting protein 1 function with regard to protein-protein interactions and levels of proteins involved in neurotransmission (M. J. Kim et al., 2016).

While the *KALRN* gene locus is not among the 108 well-established genome-wide association study loci ("Biological insights from 108 schizophrenia-associated genetic loci," 2014), it was identified in a smaller genome-wide association study (Ikeda et al., 2011). Kushima et al. identified several rare missense mutations (SNVs) in the human *KALRN* gene enriched in schizophrenia patients (Kushima et al., 2012). A global comparison of the frequencies of five selected mutations in *KALRN* between cases and control subjects showed a significant increase in frequency in schizophrenia patients (OR = 2.07, p = .003). Of these, P2255T showed a significant association with schizophrenia (OR = 2.09, p = .012), and in silico analysis via PMut predicted P2255T to be "pathological" (Kushima et al., 2012). Analysis using PolyPhen-2 software predicted that the SNV would be "benign," although this is likely accounted for by differences in the computational methods employed (Wei, Wang, Wang, Kruger, & Dunbrack, 2010). While an OR = 2 may seem small in the context of other genetic mutations, for example copy number variations, which have ORs that are several times higher, this number is highly significant in context of rare coding point mutations (Harrison, 2015). Given that none of the SNVs identified so far in exome sequencing studies (Fromer et al., 2014; Purcell et al., 2014) show statistical association

individually to schizophrenia because they are so rare, *KALRN*-P2255T stands out as one of the strongest associations of a SNV with schizophrenia identified. It is noteworthy that there is a lower-than-predicted frequency of missense SNVs in the *KALRN* gene in the Exome Aggregation Consortium database (380 observed vs. 617.5 expected; z = 4.67), which suggests that there is a constraint on mutations in the gene and indicates an important biological function for kalirin (Lek et al., 2016).

Protein and mRNA expression changes and defective kalirin signaling have been consistently reported in studies on postmortem brain tissue of schizophrenia subjects by independent laboratories. Our bioinformatics analysis further implicates kalirin signaling in molecular pathways relevant for schizophrenia. Kalirin has also been implicated in other neuropsychiatric and neurological disorders such as intellectual disability, Alzheimer's disease, impulsivity, attention-deficit/hyperactivity disorder, and ischemic stroke (Cai et al., 2014; Dang et al., 2015; DeWan et al., 2012; Horne et al., 2009; Krug et al., 2010; Lesch et al., 2008; Makrythanasis et al., 2016; L. Wang et al., 2007; Ward-Caviness et al., 2013). Therefore, it is possible that rare variants causing changes in kalirin expression or function may lead to subtle changes in neuronal function that manifest differently depending on carriers' particular genetic profiles or exposure to environmental stimuli.

The effects of kalirin-9-P2255T recapitulate some of the key dendritic phenotypes observed in schizophrenia. Reductions in dendritic length, complexity, and spine number in multiple brain regions have been well characterized in schizophrenia (Moyer, Shelton, & Sweet, 2015). Specifically, reduced basilar dendritic length and number have been described in several prefrontal

cortical areas, the anterior cingulate cortex, and the primary visual cortex (Black et al., 2004; Broadbelt et al., 2002; Glantz & Lewis, 2000; Kalus et al., 2000; Kolluri, Sun, Sampson, & Lewis, 2005; Konopaske et al., 2014). While the P2255T substitution did not alter the effects of kalirin-9 overexpression on spine density, it did prevent the increase in spine size and breadth caused by expression of kalirin-9-WT. Changes in the structure of spines as seen following kalirin-9-WT overexpression are correlated with an increase in the abundance of synaptic alpha-amino-3-hydroxy-5-methyl-4-isoxazole propionic acid (AMPA) receptors (Fu & Ip, 2017). Therefore, kalirin-9-P2255T may not be able to alter a cell's intrinsic excitability to the extent that kalirin-9-WT does. With regard to the effects of kalirin-9-P2255T on basal dendrites, it is notable that the majority of excitatory synapses on layer 5 cortical pyramidal neurons are located to the basal rather than apical dendrites (Larkman, 1991). As such, a reduction in basal dendritic complexity might be expected to give rise to the aberrant cortical circuitry that has been hypothesized to cause certain aspects of schizophrenia psychopathology (Lisman et al., 2008).

Our functional analysis reveals an unexpected compound effect on mRNA stability and intrinsic RhoA-GEF activity in kalirin-9-P2255T, unique to our knowledge among disease-associated SNVs. The effect on mRNA stability is particularly interesting. Historically, most attention has been paid to the protein sequence of disease-associated genes. However, single base-pair variations within mRNA can lead to alterations in thermodynamic stability through effects on secondary structure (Chamary & Hurst, 2005). Changes in mRNA stability, folding, and rate of degradation have been shown to be associated with human disease, independent of a change in protein sequence (Gotea, Gartner, Qutob, Elnitski, & Samuels, 2015).

As a brain-enriched dual Rac1/RhoA-GEF kalirin is in a unique position to regulate dendrite and spine morphology, as both Rac1 and RhoA are involved in dendritic growth and remodeling. Our structured illumination microscopy imaging reveals subcellular distribution differences between kalirin isoforms that are important for their functions. The kalirin-9-P2255T SNV may thus change in the balance between RhoA and Rac1 activation, leading to altered dendritic morphology. The combination of increased RhoA activation, as well as elevated kalirin-9 expression levels, may have a joint effect leading to very high elevation of downstream signaling to the cytoskeleton. Impaired signaling to the actin cytoskeleton has also been proposed as an important mechanism in the pathogenesis of schizophrenia, supported by genetic and postmortem findings, as well as in vivo models (Datta, Arion, Corradi, & Lewis, 2015; Deo et al., 2012; I. H. Kim et al., 2013; Purcell et al., 2014). Additionally, β-tubulin expression and microtubule-associated protein 2 immunoreactivity have also been shown to be decreased in schizophrenia (English, Dicker, Focking, Dunn, & Cotter, 2009; Moyer et al., 2015). Additional investigation of the P2255T variant in kalirin-9, a protein that acts in several pathways involved in cytoskeletal reorganization, could provide a platform for studying pathway perturbations that lead to schizophrenia-associated neuronal phenotypes.

CHAPTER 4: Future Directions

The research described above poses a compelling case for the role of kalirin dysfunction in the cellular abnormalities typical of schizophrenia, if not schizophrenia itself. Studies such as these are constrained by the availability of patient DNA samples, neuroimaging data, and clinical histories. An alternative method for determining the significance of kalirin in schizophrenia would be to stratify the patient group being studied along the lines of either distinct neuroanatomical phenotypes or symptom profiles, rather than treating all patients as identical with regard to diagnosis. Schizophrenia is currently considered to encompass a spectrum of disorders, varying with regard to both the incidence and severity of symptoms (Bigdeli et al., 2014; Pagsberg, 2013). The conception of the existence of discrete subtypes of schizophrenia, specifically paranoid, disorganized, catatonic, undifferentiated, and residual schizophrenia, has been abandoned with the publication of the *DSM-5* (American Psychiatric Association, 2013). The current diagnostic criteria for schizophrenia involve five key symptoms: delusions; hallucinations; disorganized speech; disorganized or catatonic behavior; and negative symptoms. Two of these five symptoms are required for a diagnosis, at least one symptom must be one of the first three. Thus, there are 23 possible combinations of symptoms, and a kalirin variant or any other risk factor could possibly only significantly associate with clinical presentation of a very specific combination of symptoms.

To raise the statistical power of studies such as those of *KALRN*-D1338N or *KALRN*-P2255T, it might also be useful to "bin" rare coding variants that occur in the same region of a gene. A recent investigation of the relative incidence of de novo coding mutations in autism spectrum disorder (ASD) and related disorders found that a statistically significant number of such mutations clustered in the region coding for the Rac-GEF domain of Trio, a protein that is

closely related to kalirin (Sadybekov, Tian, Arnesano, Katritch, & Herring, 2017). These mutations occurred in patients with ASD, intellectual disability, and other neurodevelopmental disorders, all of which are associated with abnormal dendritic spine function. Remarkably, the majority of these mutations were shown to alter both Rac1 activation in HEK 293 cells and AMPA receptor currents in hippocampal slices. Hence, this study provided proof of the principle that rare mutations can exert deleterious effects in neurons which are reminiscent of the phenotypes in the disorders in which they occur. Moreover, it raises the possibility that stronger associations between individual genes and schizophrenia might be revealed if the aggregate frequency of mutations, rather than the frequency of individual mutations, are taken into consideration.

One potential confounding issue with the current studies is that they were performed in overexpression systems, which brings the limitations of supraphysiologic expression levels. Future studies should focus on studying the variants in an endogenous setting as a model system to better elucidate potential causes of the altered neuronal morphology characteristic of schizophrenia. Introduction of the SNVs at the *Kalrn* genetic locus to generate a humanized mouse model would allow for deeper interrogation of schizophrenia-relevant pathway perturbations, as well as direct hypothesis testing of potential pharmacotherapeutic targets within these pathways. However, it is possible that because these variants lack a robust statistical association with schizophrenia and schizophrenia phenotypes, any morphological or behavioral phenotypes in knock-in mice would be subtle if they are displayed at all. In such a case it would be necessary to examine whether kalirin-related schizophrenia endophenotypes are only expressed if animals are also exposed to some sort of environmental stressor. The so-called

"two-hit hypothesis," which proposes that it is cumulative effect of multiple genetic and environmental insults, rather than individual causal factors, has been a prevailing model of schizophrenia pathogenesis (Bayer et al., 1999). Studies have shown that animals with mutations in the schizophrenia-associated Nrg1 gene display pronounced phenotypes only when also exposed to restraint stress, minimally enriched housing, or cannabis (Karl, 2013). *Kalrn* variants might then be shown to predispose to illness only in combination with specific adverse environmental factors.

Another means of exploring the effects of clinically relevant *KALRN*-D1338N or *KALRN*-P2255T gene dosage is through the use of neurons generated from carriers' induced pluripotent stem cells (iPSCs). iPSC-derived neurons from schizophrenia patients have previously been shown to display disruptions in schizophrenia-related molecular signaling pathways, and these disruptions could be reversed by treatment with an antipsychotic drug (Brennand et al., 2011). Studies of iPSC-derived neurons from patients carrying DISC1 and 22q11.2 risk alleles have also show synaptic functions and alterations in neural development which could be related to schizophrenia (Balan, Toyoshima, & Yoshikawa, 2018). If iPSC-neurons from kalirin SNV carriers display morphological and functional deficits compared with those expressing only wildtype kalirin protein, the precise impact of the SNVs could be determined more conclusively.

Finally, an approach that might be used to validate the role of kalirin-7 in schizophrenia and its potential as a drug target would be to overexpress it in the brains of mice that are considered models of the disorder. Several types of animal models are used to mimic behavioral and/or neuropathological schizophrenia endophenotypes, including those involving maternal immune

activation, post-weaning social isolation or restraint stress, and exposure to amphetamine or phencyclidine (C. A. Jones, Watson, & Fone, 2011). Given that kalirin has an essential role in dendritic spine formation and stability, as well as the expression of various cognitive phenotypes, it might be expected that in those models with deficits in dendritic spines, kalirin-7 overexpression could normalize spine function. This in turn could potentially reverse any behavioral deficits the particular animal model might display, and further validate kalirin as a prime target for therapeutic intervention.

In conclusion, the research and results described in this dissertation are not an end unto themselves. The wealth of genetic information regarding schizophrenia risk is daunting, and employing a diverse array of model systems and cellular and biochemical techniques will be necessary to assemble a clearer picture of the causes of the disorder. However, the ideas presented here reinforce the notion that genes affecting spine function are of paramount importance in the pathophysiology of schizophrenia. Furthermore, they convincingly support the concept that rare mutations can provide powerful tools for modeling disease-associated phenotypes and identifying points of convergence onto common schizophrenia-related pathways.

MATERIALS AND METHODS

Human subjects

Study participants were recruited through the Conte Center for the Neuroscience of Mental Disorders (CCNMD) at Washington University in St. Louis. Participants included individuals with schizophrenia based on Diagnostic and Statistical Manual of Mental Disorders, Ed IV (DSM-IV-TR) criteria (n = 127), and their non-affected siblings and healthy control participants (n = 246). A subset of these participants also elected to undergo structural MR imaging; their demographic information is as follows: patients (SCZ), n = 33, 9 females and 24 males, mean age of 24.3 ± 4.0 years; siblings (SCZ-SIB), n = 40, 20 females and 20 males; mean age of 23.6 ± 3.7 years; and controls (CON), n = 25, 11 females and 14 males, mean age of 20.3 ± 4.9 years. Details of the recruiting process are discussed elsewhere (Calabrese et al., 2008; Delawalla et al., 2006). All patients provided signed consent, and all activities and procedures were approved by the Washington University in St. Louis Institutional Review Board.

Genomic DNA sequencing

PCR amplification of *KALRN* exons 23-28 and adjacent intronic regions from genomic DNA samples from 127 individuals with schizophrenia and 246 siblings and controls, followed by resequencing and automated indel/SNP analysis, was performed by Beckman Coulter Genomics (Danvers, Massachusetts) on an ABI3730 capillary sequencer.

Cell culture

All procedures involving animals were approved by the Northwestern University Animal Care and Use Committee (ACUC). Animals were singly housed on a 12:12 light-dark cycle, given ad libitum access to food and water, and euthanized via CO_2 narcosis in accordance with ACUC policies. High-density cortical neuronal cultures were derived from Sprague Dawley rat E18 embryos (Envigo, Indianapolis, IN; and Charles River Laboratories, Worcester, MA). Pooled cortices were minced and cells were dissociated in a papain solution containing DNAseI, L-cysteine, and EDTA (all from Sigma-Aldrich, St. Louis, Missouri). Cells were further dissociated mechanically and then strained, followed by counting of viable cells. Neurons were plated at 3-4.5 $\times 10^5$ cells/well in 12-well plates containing poly-D-lysine (PDL)-laminin coated glass coverslips (neuVitro, Vancouver, WA) in 1 mL of plating media per well. Plating media was composed of Neurobasal Medium (Minus Phenol Red), supplemented with 2% B27 Supplement, and 2 mM GlutaMAX-I, (all from ThermoFisher Scientific, Grand Island, NY).

After 4 hours, the plating media was aspirated and replaced with B27 maintenance media (plating media plus penicillin/streptomycin (100 U/mL and 100 mg/mL, respectively; ThermoFisher). Every 3-4 days, half of the media in each well was exchanged for fresh maintenance media plus 200 μM D, L-amino-phosphonovalerate (Abcam, Cambridge, Massachusetts) was added to the media 4 days later. Neurons were incubated in a humidified chamber at 37 °C, with 5% CO_2.

HEK 293 and COS-7 cells were grown in Dulbecco's modified Eagle's medium or RPMI-1640 containing 5% fetal bovine serum (Cellgro, Manassas, VA) without antibiotics. They were grown in a humidified chamber at 37°C with 5% CO_2. They were passaged appropriately during linear growth phase to maintain sub-confluent culture. For transfections, they were seeded at 1.5×10^5

cells/well into 12-well culture-treated plates or at 6×10^5 cells/well on glass coverslips in 6-well culture-treated plates. They were grown overnight and transfected the following morning.

Transfection

The His-Myc-kalirin-7 and His-Myc-kalirin-9 plasmids were described previously (Johnson et al., 2000). PCR mutagenesis was performed with the QuikChange II Site-Directed Mutagenesis Kit (Agilent Technologies, Santa Clara, CA) to introduce the D1338N and P2255T substitutions. The sequences of the forward mutagenesis primers used to generate the substitutions were 5′-GGCAACATCCAAGAGATCTACAATTTCCATAACAACATC-3′ for kalirin-7-D1338N and 5'-AGCTGTGATCCGGTCCCAGACCCCTAGGGTTCCTCAAGC-3' for kalirin-9-P2255T. Confirmation sequencing of both plasmids was performed to verify an accurate sequence and the presence of the desired substitution. A GFP-containing plasmid was provided by Dr. Ryan Logan of the University of Pittsburgh; another, pEGFP-N2 was purchased from Clontech (Mountain View, CA). All transfections were performed using Lipofectamine LTX with Plus reagent or Lipofectamine 2000 (ThermoFisher Scientific) according to the manufacturer's protocol in the absence of antibiotics. Media was changed 4 hours after transfections for neuronal culture and 16 hours afterwards for HEK 293 cultures. For protein and mRNA half-life experiments, Actinomycin D (Sigma-Aldrich) was added to cultures at a final concentration of 10 μg/mL, and the cells were collected at T = 0, 4, or 8 hours. Cycloheximide (Sigma-Aldrich) was added at a final concentration of 400 μM and the cells were collected at T = 0, 12, 24, or 48 hours.

Western blotting

For quantification of kalirin-9 protein expression in HEK 293 cells, cell-free protein lysates were obtained from cells using radioimmune precipitation assay buffer (10 mM Tris-HCl, pH 8.0, 1 mM EDTA, pH 8.0, 0.5 mM EGTA, 140 mM NaCl, 1% Triton X-100, 0.1% sodium deoxycholate, 0.1% SDS), and total protein levels were quantified using the Lowry protein assay (Bio-Rad, Hercules, CA). 15 µg of total protein was loaded per well. Samples were electrophoresed on a NuPage Bis-Tris 4-12% gradient polyacrylamide gel (ThermoFisher Scientific) and transferred to a PVDF membrane (Millipore, Danvers, MA) at 100V for 1 hour.

For quantification of kalirin expression, membranes were blocked in Licor Blocking buffer (Odyssey, Lincoln, NE) for 1 hour at room temperature, and rabbit anti-kalirin (1:500; Millipore), mouse anti-β-tubulin (1:2000; DHSB, Iowa City, IA), and chicken anti-GFP (1:1000; Abcam) primary antibodies were added and incubated overnight at 4 °C. Membranes were washed TBS/0.1% Tween-20 and incubated with fluorophore-conjugated secondary antibodies (1:10,000) for 1 hour at room temperature. After additional washes, membranes were imaged using the Odyssey Licor System (Odyssey). Densitometric analyses were performed using MCID Core Analysis software (Imaging Research Inc., St. Catharines, Ontario, Canada).

For GTPase activation assays, transfected HEK 293 cells were harvested when they reached ~95% confluency. Active RhoA and Rac1 were isolated via GST pulldown using RhoA and Rac1 Pull-down Activation Assays (Cytoskeleton, Inc.). Protein was electrophoresed and transferred to membranes, which were then blocked in TBS/0.1% Tween-20/3% bovine serum albumin, and incubated with mouse monoclonal antibodies against either Rac1 or RhoA (1:500; Cytoskeleton

Inc., Denver, CO), c-Myc (Santa Cruz, Dallas, TX), and β-actin (1:4000, Sigma-Aldrich). They were then washed, incubated with horseradish peroxidase-conjugated secondary antibodies (1:3000), washed again, and imaged with a Gel Doc XR+ imaging system (Bio-Rad). Active RhoA and Rac1 were normalized to total RhoA and Rac1, and levels of c-Myc and β-actin expression were used to control for levels of exogenously expressed protein. ImageJ was used for quantification of band intensities (Schneider, Rasband, & Eliceiri, 2012).

Immunofluorescence, imaging, and image processing

Following transfection, neurons were fixed at either 72 hours or 14 days with cold 4% paraformaldehyde (PFA) for 20 min. They were thoroughly washed and permeabilized with PBS/0.2% Triton X-100 at room temperature for 10 min, then blocked for 20 min in PBS/0.2% Triton X-100/2% normal goat serum (Jackson ImmunoResearch Laboratories, West Grove, PA). Coverslips were incubated overnight at 4 °C with combinations of the following antibodies: mouse anti-c-Myc (1:1000; Santa Cruz Biotechnology); chicken anti-eGFP (1:10,000; Abcam); rabbit anti-kalirin-7 or kalirin-9 (1:400; (Johnson et al., 2000)); mouse anti-PSD95 (1:300; Antibodies Incorporated, Davis, CA). The following day they were washed and then incubated with Alexa Fluor 488, Alexa Fluor 568, and/or Alexa Fluor 647 secondary antibodies (Invitrogen, Carlsbad, CA) at final concentrations of 1:1000 for 1 hour at room temperature. Coverslips were then washed in PBS and mounted onto slides using Vectashield hard mounting medium (Vector Labs, Burlingame, CA) or ProLong Gold antifade reagent (ThermoFisher).

Images of healthy GFP-positive pyramidal neurons were captured at fixed exposure times in both

the 488 nm channel, and visualization of c-Myc expression in the 568 nm channel was used to ascertain kalirin overexpression. Experimenters were blinded to the genotype of the transfected plasmid throughout data acquisition and processing.

For the analysis of kalirin-9 protein expression, data acquisition was performed on an Olympus BX51 WI upright microscope (Olympus, Center Valley, PA) equipped with an Olympus spinning disk confocal. For the analyses of dendritic branching and spine morphology, images were acquired with a Zeiss LSM5 Pascal confocal microscope (Carl Zeiss Microscopy, Thornwood, NY). Images were taken under a 10× objective (N.A. 0.17), and exported to ImageJ (Schneider et al., 2012). Dendrites were traced manually, and apical dendrites, basal dendrites, and total dendritic content were analyzed using the Fiji Sholl analysis plugin. Quantitative analyses of spine number and morphology were performed as described previously (Cahill et al., 2009; K. A. Jones et al., 2009; Penzes et al., 2003; Woolfrey et al., 2009; Xie et al., 2007). Briefly, confocal images were taken using a 63× oil-immersion objective (N.A. 1.4). A Z-series of 8-12 images taken at 0.37 μm intervals were reconstructed as two-dimensional maximal projections using MetaMorph (Molecular Devices, Sunnyvale, CA). Cultures that were directly compared were stained and imaged simultaneously. For each condition, a 100 μm dendritic region from each of 10-40 neurons each from 3 experiments were analyzed.

Membrane ruffling analysis

Analysis of membrane ruffling, a process induced by actin polymerization, was performed in COS-7 cells expressing either His-Myc-kalirin-7 or His-Myc-kalirin-7-D1338N. Following fixation,

cells were immunostainied with an anti-c-Myc antibody (1:1000; Santa Cruz), and F-actin was visualized by incubation with Oregon Green 488-conjugated phalloidin (1:100; ThermoFisher). Cells expressing Myc-tagged protein were imaged using a confocal microscope (Zeiss LSM5 Pascal), and images were analyzed using ImageJ. A membrane ruffle was defined as an actin-rich undulating membrane protrusion folding back from the adherent surface of a cell.

Nissl staining of mouse brains

Mice carrying the *Kalrn* null mutation were generated by replacing exons 27 and 28 of the *Kalrn* gene with a neo cassette, and have been described previously (Cahill et al., 2009; Xie et al., 2010). Twelve-week-old mice were anesthetized with a ketamine/xylazine mixture and perfused transcardially with PBS followed by 4% PFA in PBS. Brains were removed, postfixed overnight in 4% PFA/PBS, and cryoprotected in 30% sucrose/PBS. Brains were then cryosectioned at 50 μm and mounted on slides. Slides were passed through a graded series of ethanol solutions before being stained with a solution containing 0.625% cresyl violet acetate and 0.375% acetic acid. Slides were then washed in PBS, dehydrated, and mounted with Permount (Fisher Scientific, Pittsburgh, Pennsylvania).

Cortical neuropil analysis

Cortical neuropil in mice was quantified using semiautomatic image analysis. The temporal association area from 5-6 Nissl-stained sections 300 μm apart between bregma -1.82 mm and -3.40 mm, on either side of the midline, and were imaged with a 10× objective (N.A. 0.17, lateral

resolution 0.633 μm/pixel). Analysis was performed remotely using ImageJ, with the experimenter blind to conditions. Images of layer 2/3, 4, and 5 were first thresholded to separate neurons from background. Because of possible variations in staining, images were thresholded automatically on a per-image basis. Images were then made into binary images, and glia were excluded by filtering objects smaller than 100 μm. The density of neuronal cell bodies in each image was quantified for each genotype, and neuropil size was defined as the percent of the area of each image not occupied by cell bodies. Both hemispheres from 5-6 sections were analyzed from three to four mice per genotype.

Quantitative reverse transcriptase polymerase chain reaction

Isoform-specific primers were used to detect kalirin-9 (rat origin), as well as the housekeeping gene β-actin (human origin) for normalization (kalirin-9: 5'-CCACCCAGGATGAGATGACT-3' (sense), 5'-GGTTTCTAGGAGGTGTGGGA-3' (antisense); β-actin: 5'-TTGCCAATGGTGATGACCTGGCCGT-3' (sense), 5'-CGAGCGGGAAATCGTGCGTGACATT-3' (antisense)). Real-time quantitative PCR was performed (95 °C for 10 min; [95 °C for 15 s, 60 °C for 1 min] × 40 cycles) on a Step-One Plus (Applied Biosystems, Foster City, CA) using Sybr Green (Bio-Rad) with ROX serving as the internal reference dye. Results were analyzed using the comparative Ct method.

SIM imaging and analysis

Multichannel SIM images were acquired using a Nikon Structured Illumination microscope at the

Northwestern Nikon Imaging Core using a 100× objective (N.A. 1.4). and reconstructed using Nikon Elements software and ImageJ. Single spine analyses were carried out on 98-113 spines across 15-20 neurons per condition. Acquisition was set to 10 MHz, 14 bit with EM gain and no binning. Auto exposure was kept between 100-300 ms and the EM gain multiplier restrained below 300. The reconstruction parameters Illumination Modulation Contrast (0.96), High Resolution Noise Suppression (1.19) and Out of Focus Blur Suppression (0.17) were kept constant to generate consistent images across experiments. Each dendritic segment and spine head and neck were outlined in the GFP channel.

Gene network analysis

A list of 100 *KALRN*-associated genes were predicted based on co-expression, pathway, and physical interaction, and weighted with regard to cellular component gene ontology, using the web tool on http://www.genemania.org (Warde-Farley et al., 2010). A set of 324 schizophrenia-associated genes were defined as protein coding genes residing in 108 schizophrenia-associated loci identified by GWAS ("Biological insights from 108 schizophrenia-associated genetic loci," 2014). Hypergeometric testing was performed to assess the degree of overlap between these two sets.

Statistical analyses

Comparisons between the effects of kalirin-7-WT and kalirin-7-D1338N on membrane ruffling, the effects of kalirin-9-WT and kalirin-9-P2255T on GTPase activation, kalirin-9-WT and kalirin-

9-P2255T transcript and protein levels, and *Kalrn* wildtype and heterozygous mice were performed using a two-tailed, unpaired student's t-test. Rates of kalirin-9 protein and mRNA degradation were calculated using a linear regression. Transcript half-life was determined using t1/2= ln(2)/-slope, where the slope was calculated from a plot of the log(2) normalized expression (kalirin-9 transcript relative to β-actin). For neuronal culture experiments, results were calculated with and without inclusion of experiment number as a covariate. Experiment number did not change the results and thus this covariate was not included in the final t-test. Spine parameter data were analyzed by a one-way ANOVA, followed by Bonferroni correction for multiple comparisons. Differences in Sholl analysis data were assessed by a repeated measures two-way ANOVA, followed by Bonferroni correction for multiple comparisons. All data were gathered with experimenter blinded to condition. Unblinding only occurred at time of statistical analysis.

MR image collection and processing

T1-weighted MPRAGE scans were collected on a Siemens 3T TIM TRIO imaging system (Siemens Medical Systems, Malvern, Pennsylvania) with 1 mm × 1 mm × 1 mm resolution. The MRI scans were processed with the Freesurfer (FS) image analysis suite release 4.1.0 (http://surfer.nmr.mgh.harvard.edu) (Dale, Fischl, & Sereno, 1999), which produced surface tessellations at the gray/white matter interface and the gray/CSF interface. FS provided 72 cortical regions of interest (ROI) based on a standard parcellation atlas (Desikan et al., 2006), along with measures of cortical gray matter thickness (mm) for each of these regions using embedded FS algorithms.

MR image statistical analysis

Differences between the *KALRN*-variant-bearing individual with schizophrenia (KALRN-SCZ) and schizophrenia population were evaluated by generating standard (*Z*) scores for each cortical parcellation on the cortical thickness. Significance was defined as $p < 0.05$. Due to the exploratory nature of this analysis, scores were not corrected for multiple comparisons. Sign tests were performed to determine the relative placement of the KALRN-SCZ raw score (x_K) in relation to the SCZ and CON mean values. Sign was evaluated by applying the following:

$$sign\left(\frac{x_K - \mu_{SCZ}}{\mu_{SCZ} - \mu_{CON}}\right)$$

where x_K is the KALRN-SCZ raw score, and μ_{SCZ} and μ_{CON} are the schizophrenic and control population means, respectively. If $\frac{x_K - \mu_{SCZ}}{\mu_{SCZ} - \mu_{CON}} > 0$, then sign = 1, denoting the KALRN-SCZ value for that anatomical region and measure, x_K, is further away from μ_{CON} than μ_{SCZ} is from μ_{CON} in either the positive or negative direction. If $\frac{x_K - \mu_{SCZ}}{\mu_{SCZ} - \mu_{CON}} < 0$, then sign = -1, which signified a value of x_K that is closer to μ_{CON} than μ_{SCZ} is to μ_{CON}. As we were interested in values of x_K that were accentuations of the schizophrenia phenotype, i.e. deviations from μ_{CON} in the extreme, we identified areas and measures of interest as those where $p(x_K) < 0.05$ and sign = 1.

This process was repeated to establish similar relationships between the *KALRN*-variant-bearing sibling (KALRN-SIB) and the SCZ-SIB population.

REFERENCES

Albus, M., Hubmann, W., Scherer, J., Dreikorn, B., Hecht, S., Sobizack, N., & Mohr, F. (2002). A prospective 2-year follow-up study of neurocognitive functioning in patients with first-episode schizophrenia. *Eur Arch Psychiatry Clin Neurosci, 252*(6), 262-267. doi:10.1007/s00406-002-0391-4

Alvarez, V. A., & Sabatini, B. L. (2007). Anatomical and physiological plasticity of dendritic spines. *Annu Rev Neurosci, 30*, 79-97. doi:10.1146/annurev.neuro.30.051606.094222

American Psychiatric Association. (2013). *Diagnostic and Statistical Manual of Psychiatric Disorders* (5th ed.). Arlington, VA: American Psychiatric Publishing.

Andreassen, O. A., Djurovic, S., Thompson, W. K., Schork, A. J., Kendler, K. S., O'Donovan, M. C., . . . Dale, A. M. (2013). Improved detection of common variants associated with schizophrenia by leveraging pleiotropy with cardiovascular-disease risk factors. *Am J Hum Genet, 92*(2), 197-209. doi:10.1016/j.ajhg.2013.01.001

Andreassen, O. A., Harbo, H. F., Wang, Y., Thompson, W. K., Schork, A. J., Mattingsdal, M., . . . Dale, A. M. (2015). Genetic pleiotropy between multiple sclerosis and schizophrenia but not bipolar disorder: differential involvement of immune-related gene loci. *Mol Psychiatry, 20*(2), 207-214. doi:10.1038/mp.2013.195

Balan, S., Toyoshima, M., & Yoshikawa, T. (2018). Contribution of induced pluripotent stem cell technologies to the understanding of cellular phenotypes in schizophrenia. *Neurobiol Dis*. doi:10.1016/j.nbd.2018.04.021

Barros, C. S., Calabrese, B., Chamero, P., Roberts, A. J., Korzus, E., Lloyd, K., . . . Muller, U. (2009). Impaired maturation of dendritic spines without disorganization of cortical cell layers in mice lacking NRG1/ErbB signaling in the central nervous system. *Proc Natl Acad Sci U S A, 106*(11), 4507-4512. doi:10.1073/pnas.0900355106

Bayer, T. A., Falkai, P., & Maier, W. (1999). Genetic and non-genetic vulnerability factors in schizophrenia: the basis of the "two hit hypothesis". *Journal of Psychiatric Research, 33*(6), 543-548.

Benes, F. M., & Berretta, S. (2001). GABAergic interneurons: implications for understanding schizophrenia and bipolar disorder. *Neuropsychopharmacology, 25*(1), 1-27. doi:10.1016/S0893-133X(01)00225-1

Bennett, M. R. (2011). Schizophrenia: susceptibility genes, dendritic-spine pathology and gray matter loss. *Progress in Neurobiology, 95*(3), 275-300. doi:http://dx.doi.org/10.1016/j.pneurobio.2011.08.003

Bigdeli, T. B., Bacanu, S. A., Webb, B. T., Walsh, D., O'Neill, F. A., Fanous, A. H., . . . Kendler, K. S. (2014). Molecular validation of the schizophrenia spectrum. *Schizophr Bull, 40*(1), 60-65. doi:10.1093/schbul/sbt122

Biological insights from 108 schizophrenia-associated genetic loci. (2014). *Nature, 511*(7510), 421-427. doi:10.1038/nature13595

Black, J. E., Kodish, I. M., Grossman, A. W., Klintsova, A. Y., Orlovskaya, D., Vostrikov, V., . . . Greenough, W. T. (2004). Pathology of layer V pyramidal neurons in the prefrontal cortex of patients with schizophrenia. *Am J Psychiatry, 161*(4), 742-744. doi:10.1176/appi.ajp.161.4.742

Branco, T., & Hausser, M. (2011). Synaptic integration gradients in single cortical pyramidal cell dendrites. *Neuron, 69*(5), 885-892. doi:10.1016/j.neuron.2011.02.006

Brauns, S., Gollub, R. L., Roffman, J. L., Yendiki, A., Ho, B. C., Wassink, T. H., . . . Ehrlich, S. (2011). DISC1 is associated with cortical thickness and neural efficiency. *Neuroimage, 57*(4), 1591-1600. doi:10.1016/j.neuroimage.2011.05.058

Brennand, K. J., Simone, A., Jou, J., Gelboin-Burkhart, C., Tran, N., Sangar, S., . . . Gage, F. H. (2011). Modelling schizophrenia using human induced pluripotent stem cells. *Nature, 473*(7346), 221-225. doi:10.1038/nature09915

Broadbelt, K., Byne, W., & Jones, L. B. (2002). Evidence for a decrease in basilar dendrites of pyramidal cells in schizophrenic medial prefrontal cortex. *Schizophr Res, 58*(1), 75-81.

Bromet, E. J., & Fennig, S. (1999). Epidemiology and natural history of schizophrenia. *Biol Psychiatry, 46*(7), 871-881.

Brunet-Gouet, E., Achim, A. M., Vistoli, D., Passerieux, C., Hardy-Bayle, M. C., & Jackson, P. L. (2011). The study of social cognition with neuroimaging methods as a means to explore future directions of deficit evaluation in schizophrenia? *Psychiatry Res, 190*(1), 23-31. doi:10.1016/j.psychres.2010.11.029

Buxbaum, J. D. (2009). Multiple rare variants in the etiology of autism spectrum disorders. *Dialogues Clin Neurosci, 11*(1), 35-43.

Cahill, M. E., Remmers, C., Jones, K. A., Xie, Z., Sweet, R. A., & Penzes, P. (2013). Neuregulin1 signaling promotes dendritic spine growth through kalirin. *J Neurochem, 126*(5), 625-635. doi:10.1111/jnc.12330

Cahill, M. E., Xie, Z., Day, M., Photowala, H., Barbolina, M. V., Miller, C. A., . . . Penzes, P. (2009). Kalirin regulates cortical spine morphogenesis and disease-related behavioral phenotypes. *Proc Natl Acad Sci U S A, 106*(31), 13058-13063. doi:10.1073/pnas.0904636106

Cai, D. C., Fonteijn, H., Guadalupe, T., Zwiers, M., Wittfeld, K., Teumer, A., . . . Hagoort, P. (2014). A genome-wide search for quantitative trait loci affecting the cortical surface area and thickness of Heschl's gyrus. *Genes, Brain, & Behavior, 13*(7), 675-685.

doi:10.1111/gbb.12157

Calabrese, D. R., Wang, L., Harms, M. P., Ratnanather, J. T., Barch, D. M., Cloninger, C. R., . . . Csernansky, J. G. (2008). Cingulate gyrus neuroanatomy in schizophrenia subjects and their non-psychotic siblings. *Schizophr Res, 104*(1-3), 61-70. doi:10.1016/j.schres.2008.06.014

Cannon, T. D., Hennah, W., van Erp, T. G., Thompson, P. M., Lonnqvist, J., Huttunen, M., . . . Peltonen, L. (2005). Association of DISC1/TRAX haplotypes with schizophrenia, reduced prefrontal gray matter, and impaired short- and long-term memory. *Arch Gen Psychiatry, 62*(11), 1205-1213. doi:10.1001/archpsyc.62.11.1205

Carless, M. A., Glahn, D. C., Johnson, M. P., Curran, J. E., Bozaoglu, K., Dyer, T. D., . . . Blangero, J. (2011). Impact of DISC1 variation on neuroanatomical and neurocognitive phenotypes. *Mol Psychiatry, 16*(11), 1096-1104, 1063. doi:10.1038/mp.2011.37

Casanova, M. F. (1997). Functional and anatomical aspects of prefrontal pathology in schizophrenia. *Schizophr Bull, 23*(3), 517-519.

Caspi, A., Reichenberg, A., Weiser, M., Rabinowitz, J., Kaplan, Z., Knobler, H., . . . Davidson, M. (2003). Cognitive performance in schizophrenia patients assessed before and following the first psychotic episode. *Schizophr Res, 65*(2-3), 87-94.

Chamary, J. V., & Hurst, L. D. (2005). Evidence for selection on synonymous mutations affecting stability of mRNA secondary structure in mammals. *Genome Biol, 6*(9), R75. doi:10.1186/gb-2005-6-9-r75

Cherfils, J., & Zeghouf, M. (2013). Regulation of small GTPases by GEFs, GAPs, and GDIs. *Physiol Rev, 93*(1), 269-309. doi:10.1152/physrev.00003.2012

Cotter, D., Wilson, S., Roberts, E., Kerwin, R., & Everall, I. P. (2000). Increased dendritic MAP2

expression in the hippocampus in schizophrenia. *Schizophr Res, 41*(2), 313-323.

Cross-Disorder Group of the Psychiatric Genomics, C. (2013). Identification of risk loci with shared effects on five major psychiatric disorders: a genome-wide analysis. *Lancet, 381*(9875), 1371-1379. doi:10.1016/S0140-6736(12)62129-1

Cross-Disorder Group of the Psychiatric Genomics, C., Lee, S. H., Ripke, S., Neale, B. M., Faraone, S. V., Purcell, S. M., . . . International Inflammatory Bowel Disease Genetics, C. (2013). Genetic relationship between five psychiatric disorders estimated from genome-wide SNPs. *Nat Genet, 45*(9), 984-994. doi:10.1038/ng.2711

Cullen, P. J., & Korswagen, H. C. (2011). Sorting nexins provide diversity for retromer-dependent trafficking events. *Nat Cell Biol, 14*(1), 29-37. doi:10.1038/ncb2374

Dale, A. M., Fischl, B., & Sereno, M. I. (1999). Cortical surface-based analysis. I. Segmentation and surface reconstruction. *Neuroimage, 9*(2), 179-194. doi:10.1006/nimg.1998.0395

Dang, M., Wang, Z., Zhang, R., Li, X., Peng, Y., Han, X., . . . Tian, J. (2015). KALRN Rare and Common Variants and Susceptibility to Ischemic Stroke in Chinese Han Population. *Neuromolecular Med, 17*(3), 241-250. doi:10.1007/s12017-015-8352-z

Datta, D., Arion, D., Corradi, J. P., & Lewis, D. A. (2015). Altered expression of CDC42 signaling pathway components in cortical layer 3 pyramidal cells in schizophrenia. *Biol Psychiatry, 78*(11), 775-785. doi:10.1016/j.biopsych.2015.03.030

Dean, B. (2009). Interpreting the significance of decreased cortical serotonin 2A receptors in schizophrenia. *Prog Neuropsychopharmacol Biol Psychiatry, 33*(8), 1583-1584; author reply 1585-1586. doi:10.1016/j.pnpbp.2009.08.006

Delawalla, Z., Barch, D. M., Fisher Eastep, J. L., Thomason, E. S., Hanewinkel, M. J., Thompson, P. A., & Csernansky, J. G. (2006). Factors mediating cognitive deficits and

psychopathology among siblings of individuals with schizophrenia. *Schizophr Bull, 32*(3), 525-537. doi:10.1093/schbul/sbj082

Deo, A. J., Cahill, M. E., Li, S., Goldszer, I., Henteleff, R., Vanleeuwen, J. E., . . . Sweet, R. A. (2012). Increased expression of Kalirin-9 in the auditory cortex of schizophrenia subjects: its role in dendritic pathology. *Neurobiol Dis, 45*(2), 796-803. doi:10.1016/j.nbd.2011.11.003

Desikan, R. S., Segonne, F., Fischl, B., Quinn, B. T., Dickerson, B. C., Blacker, D., . . . Killiany, R. J. (2006). An automated labeling system for subdividing the human cerebral cortex on MRI scans into gyral based regions of interest. *Neuroimage, 31*(3), 968-980. doi:S1053-8119(06)00043-7 [pii]

10.1016/j.neuroimage.2006.01.021

DeWan, A. T., Egan, K. B., Hellenbrand, K., Sorrentino, K., Pizzoferrato, N., Walsh, K. M., & Bracken, M. B. (2012). Whole-exome sequencing of a pedigree segregating asthma. *BMC Med Genet, 13*, 95. doi:10.1186/1471-2350-13-95

Donaldson, J. G., & Jackson, C. L. (2011). ARF family G proteins and their regulators: roles in membrane transport, development and disease. *Nat Rev Mol Cell Biol, 12*(6), 362-375. doi:10.1038/nrm3117

Duan, J., Sanders, A. R., & Gejman, P. V. (2010). Genome-wide approaches to schizophrenia. *Brain Research Bulletin, 83*(3-4), 93-102. doi:10.1016/j.brainresbull.2010.04.009

Duan, J., Wainwright, M. S., Comeron, J. M., Saitou, N., Sanders, A. R., Gelernter, J., & Gejman, P. V. (2003). Synonymous mutations in the human dopamine receptor D2 (DRD2) affect mRNA stability and synthesis of the receptor. *Hum Mol Genet, 12*(3), 205-216.

Duman, J. G., Mulherkar, S., Tu, Y. K., J, X. C., & Tolias, K. F. (2015). Mechanisms for

spatiotemporal regulation of Rho-GTPase signaling at synapses. *Neurosci Lett, 601*, 4-10. doi:10.1016/j.neulet.2015.05.034

English, J. A., Dicker, P., Focking, M., Dunn, M. J., & Cotter, D. R. (2009). 2-D DIGE analysis implicates cytoskeletal abnormalities in psychiatric disease. *Proteomics, 9*(12), 3368-3382. doi:10.1002/pmic.200900015

Fiala, J. C., Spacek, J., & Harris, K. M. (2002). Dendritic spine pathology: cause or consequence of neurological disorders? *Brain Res Brain Res Rev, 39*(1), 29-54.

Fromer, M., Pocklington, A. J., Kavanagh, D. H., Williams, H. J., Dwyer, S., Gormley, P., . . . O'Donovan, M. C. (2014). De novo mutations in schizophrenia implicate synaptic networks. *Nature, 506*(7487), 179-184. doi:10.1038/nature12929

Fu, A. K., & Ip, N. Y. (2017). Regulation of postsynaptic signaling in structural synaptic plasticity. *Curr Opin Neurobiol, 45*, 148-155. doi:10.1016/j.conb.2017.05.016

Gejman, P. V., Sanders, A. R., & Duan, J. (2010). The role of genetics in the etiology of schizophrenia. *Psychiatr Clin North Am, 33*(1), 35-66. doi:10.1016/j.psc.2009.12.003

Glantz, L. A., & Lewis, D. A. (2000). Decreased dendritic spine density on prefrontal cortical pyramidal neurons in schizophrenia. *Arch Gen Psychiatry, 57*(1), 65-73.

Glausier, J. R., & Lewis, D. A. (2013). Dendritic spine pathology in schizophrenia. *Neuroscience, 251*, 90-107. doi:http://dx.doi.org/10.1016/j.neuroscience.2012.04.044

Glessner, J. T., Reilly, M. P., Kim, C. E., Takahashi, N., Albano, A., Hou, C., . . . Hakonarson, H. (2010). Strong synaptic transmission impact by copy number variations in schizophrenia. *Proc Natl Acad Sci U S A, 107*(23), 10584-10589. doi:1000274107 [pii]

10.1073/pnas.1000274107

Goldman-Rakic, P. S., & Selemon, L. D. (1997). Functional and anatomical aspects of prefrontal

pathology in schizophrenia. *Schizophr Bull, 23*(3), 437-458.

Gonzalez-Jamett, A. M., Momboisse, F., Haro-Acuna, V., Bevilacqua, J. A., Caviedes, P., & Cardenas, A. M. (2013). Dynamin-2 function and dysfunction along the secretory pathway. *Front Endocrinol (Lausanne), 4*, 126. doi:10.3389/fendo.2013.00126

Gordon, U., Polsky, A., & Schiller, J. (2006). Plasticity compartments in basal dendrites of neocortical pyramidal neurons. *J Neurosci, 26*(49), 12717-12726. doi:10.1523/JNEUROSCI.3502-06.2006

Gotea, V., Gartner, J. J., Qutob, N., Elnitski, L., & Samuels, Y. (2015). The functional relevance of somatic synonymous mutations in melanoma and other cancers. *Pigment Cell Melanoma Res, 28*(6), 673-684. doi:10.1111/pcmr.12413

Govek, E. E., Newey, S. E., Akerman, C. J., Cross, J. R., Van der Veken, L., & Van Aelst, L. (2004). The X-linked mental retardation protein oligophrenin-1 is required for dendritic spine morphogenesis. *Nat Neurosci, 7*(4), 364-372. doi:10.1038/nn1210

Green, M. F. (1996). What are the functional consequences of neurocognitive deficits in schizophrenia? *Am J Psychiatry, 153*(3), 321-330. doi:10.1176/ajp.153.3.321

Guilluy, C., Garcia-Mata, R., & Burridge, K. (2011). Rho protein crosstalk: another social network? *Trends Cell Biol, 21*(12), 718-726. doi:10.1016/j.tcb.2011.08.002

Gur, R. E., Kohler, C. G., Ragland, J. D., Siegel, S. J., Lesko, K., Bilker, W. B., & Gur, R. C. (2006). Flat affect in schizophrenia: relation to emotion processing and neurocognitive measures. *Schizophr Bull, 32*(2), 279-287. doi:10.1093/schbul/sbj041

Gustafsson, M. G. (2005). Nonlinear structured-illumination microscopy: wide-field fluorescence imaging with theoretically unlimited resolution. *Proc Natl Acad Sci U S A, 102*(37), 13081-13086. doi:10.1073/pnas.0406877102

Hall, A. (1998). Rho GTPases and the actin cytoskeleton. *Science, 279*(5350), 509-514.

Hall, J., Trent, S., Thomas, K. L., O'Donovan, M. C., & Owen, M. J. (2015). Genetic risk for schizophrenia: convergence on synaptic pathways involved in plasticity. *Biol Psychiatry, 77*(1), 52-58. doi:10.1016/j.biopsych.2014.07.011

Harris, K. M. (1999). Structure, development, and plasticity of dendritic spines. *Curr Opin Neurobiol, 9*(3), 343-348.

Harrison, P. J. (2015). The current and potential impact of genetics and genomics on neuropsychopharmacology. *Eur Neuropsychopharmacol, 25*(5), 671-681. doi:10.1016/j.euroneuro.2013.02.005

Harvey, I., Ron, M. A., Du Boulay, G., Wicks, D., Lewis, S. W., & Murray, R. M. (1993). Reduction of cortical volume in schizophrenia on magnetic resonance imaging. *Psychol Med, 23*(3), 591-604.

Hayashi-Takagi, A., Takaki, M., Graziane, N., Seshadri, S., Murdoch, H., Dunlop, A. J., . . . Sawa, A. (2010). Disrupted-in-Schizophrenia 1 (DISC1) regulates spines of the glutamate synapse via Rac1. *Nat Neurosci, 13*(3), 327-332. doi:10.1038/nn.2487

Hedrick, N. G., Harward, S. C., Hall, C. E., Murakoshi, H., McNamara, J. O., & Yasuda, R. (2016). Rho GTPase complementation underlies BDNF-dependent homo- and heterosynaptic plasticity. *Nature, 538*(7623), 104-108. doi:10.1038/nature19784

Henley, J. M., & Wilkinson, K. A. (2016). Synaptic AMPA receptor composition in development, plasticity and disease. *Nat Rev Neurosci, 17*(6), 337-350. doi:10.1038/nrn.2016.37

Herz, M. I., & Melville, C. (1980). Relapse in schizophrenia. *Am J Psychiatry, 137*(7), 801-805. doi:10.1176/ajp.137.7.801

Hill, J. J., Hashimoto, T., & Lewis, D. A. (2006). Molecular mechanisms contributing to dendritic

spine alterations in the prefrontal cortex of subjects with schizophrenia. *Mol Psychiatry, 11*(6), 557-566. doi:10.1038/sj.mp.4001792

Horne, B. D., Hauser, E. R., Wang, L., Muhlestein, J. B., Anderson, J. L., Carlquist, J. F., . . . Kraus, W. E. (2009). Validation study of genetic associations with coronary artery disease on chromosome 3q13-21 and potential effect modification by smoking. *Ann Hum Genet, 73*(Pt 6), 551-558. doi:10.1111/j.1469-1809.2009.00540.x

Human Genome Structural Variation Working, G., Eichler, E. E., Nickerson, D. A., Altshuler, D., Bowcock, A. M., Brooks, L. D., . . . Waterston, R. H. (2007). Completing the map of human genetic variation. *Nature, 447*(7141), 161-165. doi:10.1038/447161a

Hutsler, J. J., & Zhang, H. (2010). Increased dendritic spine densities on cortical projection neurons in autism spectrum disorders. *Brain Res, 1309*, 83-94. doi:S0006-8993(09)02311-7 [pii]

10.1016/j.brainres.2009.09.120

Huttenlocher, P. R. (1979). Synaptic density in human frontal cortex - developmental changes and effects of aging. *Brain Res, 163*(2), 195-205.

Iafrate, A. J., Feuk, L., Rivera, M. N., Listewnik, M. L., Donahoe, P. K., Qi, Y., . . . Lee, C. (2004). Detection of large-scale variation in the human genome. *Nat Genet, 36*(9), 949-951. doi:10.1038/ng1416

Ikeda, M., Aleksic, B., Kinoshita, Y., Okochi, T., Kawashima, K., Kushima, I., . . . Iwata, N. (2011). Genome-wide association study of schizophrenia in a Japanese population. *Biol Psychiatry, 69*(5), 472-478. doi:10.1016/j.biopsych.2010.07.010

Iossifov, I., O'Roak, B. J., Sanders, S. J., Ronemus, M., Krumm, N., Levy, D., . . . Wigler, M. (2014). The contribution of de novo coding mutations to autism spectrum disorder. *Nature*,

515(7526), 216-221. doi:10.1038/nature13908

Irwin, S. A., Galvez, R., & Greenough, W. T. (2000). Dendritic spine structural anomalies in fragile-X mental retardation syndrome. *Cereb Cortex, 10*(10), 1038-1044.

Isshiki, M., Tanaka, S., Kuriu, T., Tabuchi, K., Takumi, T., & Okabe, S. (2014). Enhanced synapse remodelling as a common phenotype in mouse models of autism. *Nat Commun, 5*, 4742. doi:10.1038/ncomms5742

Ito, H., Morishita, R., Shinoda, T., Iwamoto, I., Sudo, K., Okamoto, K., & Nagata, K. (2010). Dysbindin-1, WAVE2 and Abi-1 form a complex that regulates dendritic spine formation. *Mol Psychiatry, 15*(10), 976-986. doi:10.1038/mp.2010.69

Johnson, R. C., Penzes, P., Eipper, B. A., & Mains, R. E. (2000). Isoforms of kalirin, a neuronal Dbl family member, generated through use of different 5'- and 3'-ends along with an internal translational initiation site. *J Biol Chem, 275*(25), 19324-19333. doi:10.1074/jbc.M000676200

Jones, C. A., Watson, D. J., & Fone, K. C. (2011). Animal models of schizophrenia. *Br J Pharmacol, 164*(4), 1162-1194. doi:10.1111/j.1476-5381.2011.01386.x

Jones, K. A., Srivastava, D. P., Allen, J. A., Strachan, R. T., Roth, B. L., & Penzes, P. (2009). Rapid modulation of spine morphology by the 5-HT2A serotonin receptor through kalirin-7 signaling. *Proc Natl Acad Sci U S A, 106*(46), 19575-19580. doi:0905884106 [pii]

10.1073/pnas.0905884106

Jones, P., Rodgers, B., Murray, R., & Marmot, M. (1994). Child development risk factors for adult schizophrenia in the British 1946 birth cohort. *Lancet, 344*(8934), 1398-1402.

Kalus, P., Muller, T. J., Zuschratter, W., & Senitz, D. (2000). The dendritic architecture of prefrontal pyramidal neurons in schizophrenic patients. *Neuroreport, 11*(16), 3621-3625.

Karl, T. (2013). Neuregulin 1: a prime candidate for research into gene-environment interactions in schizophrenia? Insights from genetic rodent models. *Front Behav Neurosci, 7*, 106. doi:10.3389/fnbeh.2013.00106

Karlsgodt, K. H., Sun, D., Jimenez, A. M., Lutkenhoff, E. S., Willhite, R., van Erp, T. G., & Cannon, T. D. (2008). Developmental disruptions in neural connectivity in the pathophysiology of schizophrenia. *Dev Psychopathol, 20*(4), 1297-1327. doi:10.1017/S095457940800062X

Keefe, R. S., Bilder, R. M., Davis, S. M., Harvey, P. D., Palmer, B. W., Gold, J. M., . . . Neurocognitive Working, G. (2007). Neurocognitive effects of antipsychotic medications in patients with chronic schizophrenia in the CATIE Trial. *Arch Gen Psychiatry, 64*(6), 633-647. doi:10.1001/archpsyc.64.6.633

Kim, I. H., Racz, B., Wang, H., Burianek, L., Weinberg, R., Yasuda, R., . . . Soderling, S. H. (2013). Disruption of Arp2/3 results in asymmetric structural plasticity of dendritic spines and progressive synaptic and behavioral abnormalities. *J Neurosci, 33*(14), 6081-6092. doi:10.1523/JNEUROSCI.0035-13.2013

Kim, M. J., Biag, J., Fass, D. M., Lewis, M. C., Zhang, Q., Fleishman, M., . . . Haggarty, S. J. (2016). Functional analysis of rare variants found in schizophrenia implicates a critical role for GIT1-PAK3 signaling in neuroplasticity. *Mol Psychiatry*. doi:10.1038/mp.2016.98

Kolluri, N., Sun, Z., Sampson, A. R., & Lewis, D. A. (2005). Lamina-specific reductions in dendritic spine density in the prefrontal cortex of subjects with schizophrenia. *Am J Psychiatry, 162*(6), 1200-1202. doi:10.1176/appi.ajp.162.6.1200

Kolomeets, N. S., Orlovskaya, D. D., Rachmanova, V. I., & Uranova, N. A. (2005). Ultrastructural alterations in hippocampal mossy fiber synapses in schizophrenia: a postmortem

morphometric study. *Synapse, 57*(1), 47-55. doi:10.1002/syn.20153

Konopaske, G. T., Lange, N., Coyle, J. T., & Benes, F. M. (2014). Prefrontal cortical dendritic spine pathology in schizophrenia and bipolar disorder. *JAMA Psychiatry, 71*(12), 1323-1331. doi:10.1001/jamapsychiatry.2014.1582

Koo, T. H., Eipper, B. A., & Donaldson, J. G. (2007). Arf6 recruits the Rac GEF Kalirin to the plasma membrane facilitating Rac activation. *BMC Cell Biol, 8*, 29. doi:10.1186/1471-2121-8-29

Krug, T., Manso, H., Gouveia, L., Sobral, J., Xavier, J. M., Albergaria, I., . . . Oliveira, S. A. (2010). Kalirin: a novel genetic risk factor for ischemic stroke. *Hum Genet, 127*(5), 513-523. doi:10.1007/s00439-010-0790-y

Kryukov, G. V., Pennacchio, L. A., & Sunyaev, S. R. (2007). Most rare missense alleles are deleterious in humans: implications for complex disease and association studies. *Am J Hum Genet, 80*(4), 727-739. doi:S0002-9297(07)61104-5 [pii]

10.1086/513473

Kushima, I., Nakamura, Y., Aleksic, B., Ikeda, M., Ito, Y., Shiino, T., . . . Ozaki, N. (2012). Resequencing and association analysis of the KALRN and EPHB1 genes and their contribution to schizophrenia susceptibility. *Schizophr Bull, 38*(3), 552-560. doi:10.1093/schbul/sbq118

Lai, K. O., & Ip, N. Y. (2013). Structural plasticity of dendritic spines: the underlying mechanisms and its dysregulation in brain disorders. *Biochim Biophys Acta, 1832*(12), 2257-2263. doi:10.1016/j.bbadis.2013.08.012

Lamprecht, R., & LeDoux, J. (2004). Structural plasticity and memory. *Nat Rev Neurosci, 5*(1), 45-54. doi:10.1038/nrn1301

Larkman, A. U. (1991). Dendritic morphology of pyramidal neurones of the visual cortex of the rat: III. Spine distributions. *J Comp Neurol, 306*(2), 332-343. doi:10.1002/cne.903060209

Lee, F. H., Fadel, M. P., Preston-Maher, K., Cordes, S. P., Clapcote, S. J., Price, D. J., . . . Wong, A. H. (2011). Disc1 point mutations in mice affect development of the cerebral cortex. *J Neurosci, 31*(9), 3197-3206. doi:10.1523/JNEUROSCI.4219-10.2011

Lek, M., Karczewski, K. J., Minikel, E. V., Samocha, K. E., Banks, E., Fennell, T., . . . MacArthur, D. G. (2016). Analysis of protein-coding genetic variation in 60,706 humans. *Nature, 536*(7616), 285-291. doi:10.1038/nature19057

Lennox, A. L., Mao, H., & Silver, D. L. (2017). RNA on the brain: emerging layers of post-transcriptional regulation in cerebral cortex development. *Wiley Interdiscip Rev Dev Biol*. doi:10.1002/wdev.290

Lepagnol-Bestel, A. M., Kvajo, M., Karayiorgou, M., Simonneau, M., & Gogos, J. A. (2013). A Disc1 mutation differentially affects neurites and spines in hippocampal and cortical neurons. *Mol Cell Neurosci, 54*, 84-92. doi:10.1016/j.mcn.2013.01.006

Lesch, K. P., Timmesfeld, N., Renner, T. J., Halperin, R., Roser, C., Nguyen, T. T., . . . Jacob, C. (2008). Molecular genetics of adult ADHD: converging evidence from genome-wide association and extended pedigree linkage studies. *J Neural Transm (Vienna), 115*(11), 1573-1585. doi:10.1007/s00702-008-0119-3

Lewis, D. A., & Sweet, R. A. (2009). Schizophrenia from a neural circuitry perspective: advancing toward rational pharmacological therapies. *J Clin Invest, 119*(4), 706-716. doi:10.1172/JCI37335

Li, N., Lee, B., Liu, R. J., Banasr, M., Dwyer, J. M., Iwata, M., . . . Duman, R. S. (2010). mTOR-dependent synapse formation underlies the rapid antidepressant effects of NMDA

antagonists. *Science, 329*(5994), 959-964. doi:10.1126/science.1190287

Lieberman, J. A., Stroup, T. S., McEvoy, J. P., Swartz, M. S., Rosenheck, R. A., Perkins, D. O., . . . Clinical Antipsychotic Trials of Intervention Effectiveness, I. (2005). Effectiveness of antipsychotic drugs in patients with chronic schizophrenia. *N Engl J Med, 353*(12), 1209-1223. doi:10.1056/NEJMoa051688

Lisman, J. E., Coyle, J. T., Green, R. W., Javitt, D. C., Benes, F. M., Heckers, S., & Grace, A. A. (2008). Circuit-based framework for understanding neurotransmitter and risk gene interactions in schizophrenia. *Trends Neurosci, 31*(5), 234-242. doi:10.1016/j.tins.2008.02.005

Ma, X. M., Huang, J. P., Xin, X., Yan, Y., Mains, R. E., & Eipper, B. A. (2012). A role for kalirin in the response of rat medium spiny neurons to cocaine. *Mol Pharmacol, 82*(4), 738-745. doi:10.1124/mol.112.080044

Ma, X. M., Kiraly, D. D., Gaier, E. D., Wang, Y., Kim, E. J., Levine, E. S., . . . Mains, R. E. (2008). Kalirin-7 is required for synaptic structure and function. *J Neurosci, 28*(47), 12368-12382. doi:10.1523/JNEUROSCI.4269-08.2008

MacDonald, M. L., Alhassan, J., Newman, J. T., Richard, M., Gu, H., Kelly, R. M., . . . Sweet, R. A. (2017). Selective Loss of Smaller Spines in Schizophrenia. *Am J Psychiatry, 174*(6), 586-594. doi:10.1176/appi.ajp.2017.16070814

Makrythanasis, P., Guipponi, M., Santoni, F. A., Zaki, M., Issa, M. Y., Ansar, M., . . . Antonarakis, S. E. (2016). Exome sequencing discloses KALRN homozygous variant as likely cause of intellectual disability and short stature in a consanguineous pedigree. *Hum Genomics, 10*(1), 26. doi:10.1186/s40246-016-0082-2

Marshall, C. R., Howrigan, D. P., Merico, D., Thiruvahindrapuram, B., Wu, W., Greer, D. S., . . .

Schizophrenia Working Groups of the Psychiatric Genomics, C. (2017). Contribution of copy number variants to schizophrenia from a genome-wide study of 41,321 subjects. *Nat Genet, 49*(1), 27-35. doi:10.1038/ng.3725

Mavroudis, I. A., Fotiou, D. F., Manani, M. G., Njaou, S. N., Frangou, D., Costa, V. G., & Baloyannis, S. J. (2011). Dendritic pathology and spinal loss in the visual cortex in Alzheimer's disease: a Golgi study in pathology. *Int J Neurosci, 121*(7), 347-354. doi:10.3109/00207454.2011.553753

Maynard, T. M., Sikich, L., Lieberman, J. A., & LaMantia, A. S. (2001). Neural development, cell-cell signaling, and the "two-hit" hypothesis of schizophrenia. *Schizophr Bull, 27*(3), 457-476.

Meda, S. A., Ruano, G., Windemuth, A., O'Neil, K., Berwise, C., Dunn, S. M., . . . Pearlson, G. D. (2014). Multivariate analysis reveals genetic associations of the resting default mode network in psychotic bipolar disorder and schizophrenia. *Proc Natl Acad Sci U S A, 111*(19), E2066-2075. doi:10.1073/pnas.1313093111

Meltzer, H. Y., Massey, B. W., & Horiguchi, M. (2012). Serotonin receptors as targets for drugs useful to treat psychosis and cognitive impairment in schizophrenia. *Curr Pharm Biotechnol, 13*(8), 1572-1586.

Meng, Y., Zhang, Y., Tregoubov, V., Janus, C., Cruz, L., Jackson, M., . . . Jia, Z. (2002). Abnormal spine morphology and enhanced LTP in LIMK-1 knockout mice. *Neuron, 35*(1), 121-133.

Mizuki, Y., Takaki, M., Sakamoto, S., Okamoto, S., Kishimoto, M., Okahisa, Y., . . . Yamada, N. (2016). Human Rho Guanine Nucleotide Exchange Factor 11 (ARHGEF11) Regulates Dendritic Morphogenesis. *Int J Mol Sci, 18*(1). doi:10.3390/ijms18010067

Morrow, E. M., Kane, A., Goff, D. C., & Walsh, C. A. (2008). Sequence analysis of P21-activated

kinase 3 (PAK3) in chronic schizophrenia with cognitive impairment. *Schizophr Res, 106*(2-3), 265-267. doi:10.1016/j.schres.2008.08.021

Moyer, C. E., Shelton, M. A., & Sweet, R. A. (2015). Dendritic spine alterations in schizophrenia. *Neurosci Lett, 601,* 46-53. doi:10.1016/j.neulet.2014.11.042

Mulle, J. G., Dodd, A. F., McGrath, J. A., Wolyniec, P. S., Mitchell, A. A., Shetty, A. C., . . . Warren, S. T. (2010). Microdeletions of 3q29 confer high risk for schizophrenia. *Am J Hum Genet, 87*(2), 229-236. doi:10.1016/j.ajhg.2010.07.013

Myers, R. A., Casals, F., Gauthier, J., Hamdan, F. F., Keebler, J., Boyko, A. R., . . . Awadalla, P. (2011). A population genetic approach to mapping neurological disorder genes using deep resequencing. *PLoS Genet, 7*(2), e1001318. doi:10.1371/journal.pgen.1001318

Nakayama, A. Y., Harms, M. B., & Luo, L. (2000). Small GTPases Rac and Rho in the maintenance of dendritic spines and branches in hippocampal pyramidal neurons. *J Neurosci, 20*(14), 5329-5338.

Owen, M. J., O'Donovan, M. C., Thapar, A., & Craddock, N. (2011). Neurodevelopmental hypothesis of schizophrenia. *Br J Psychiatry, 198*(3), 173-175. doi:10.1192/bjp.bp.110.084384

Pagsberg, A. K. (2013). Schizophrenia spectrum and other psychotic disorders. *Eur Child Adolesc Psychiatry, 22 Suppl 1,* S3-9. doi:10.1007/s00787-012-0354-x

Pakkenberg, B. (1993). Total nerve cell number in neocortex in chronic schizophrenics and controls estimated using optical disectors. *Biol Psychiatry, 34*(11), 768-772.

Penzes, P., Beeser, A., Chernoff, J., Schiller, M. R., Eipper, B. A., Mains, R. E., & Huganir, R. L. (2003). Rapid induction of dendritic spine morphogenesis by trans-synaptic ephrinB-EphB receptor activation of the Rho-GEF kalirin. *Neuron, 37*(2), 263-274.

Penzes, P., & Cahill, M. E. (2012). Deconstructing signal transduction pathways that regulate the actin cytoskeleton in dendritic spines. *Cytoskeleton (Hoboken), 69*(7), 426-441. doi:10.1002/cm.21015

Penzes, P., Cahill, M. E., Jones, K. A., VanLeeuwen, J. E., & Woolfrey, K. M. (2011). Dendritic spine pathology in neuropsychiatric disorders. *Nat Neurosci, 14*(3), 285-293. doi:nn.2741 [pii]

10.1038/nn.2741

Penzes, P., Johnson, R. C., Alam, M. R., Kambampati, V., Mains, R. E., & Eipper, B. A. (2000). An isoform of kalirin, a brain-specific GDP/GTP exchange factor, is enriched in the postsynaptic density fraction. *J Biol Chem, 275*(9), 6395-6403.

Penzes, P., Johnson, R. C., Kambampati, V., Mains, R. E., & Eipper, B. A. (2001). Distinct roles for the two Rho GDP/GTP exchange factor domains of kalirin in regulation of neurite growth and neuronal morphology. *J Neurosci, 21*(21), 8426-8434.

Penzes, P., & Jones, K. A. (2008). Dendritic spine dynamics--a key role for kalirin-7. *Trends Neurosci, 31*(8), 419-427. doi:S0166-2236(08)00146-X [pii]

10.1016/j.tins.2008.06.001

Penzes, P., & Rafalovich, I. (2012). Regulation of the actin cytoskeleton in dendritic spines. *Adv Exp Med Biol, 970*, 81-95. doi:10.1007/978-3-7091-0932-8_4

Petrak, L. J., Harris, K. M., & Kirov, S. A. (2005). Synaptogenesis on mature hippocampal dendrites occurs via filopodia and immature spines during blocked synaptic transmission. *J Comp Neurol, 484*(2), 183-190. doi:10.1002/cne.20468

Pick, J. E., & Ziff, E. B. (2018). Regulation of AMPA receptor trafficking and exit from the endoplasmic reticulum. *Mol Cell Neurosci*. doi:10.1016/j.mcn.2018.03.004

Prosser, D. C., Tran, D., Schooley, A., Wendland, B., & Ngsee, J. K. (2010). A novel, retromer-independent role for sorting nexins 1 and 2 in RhoG-dependent membrane remodeling. *Traffic, 11*(10), 1347-1362. doi:10.1111/j.1600-0854.2010.01100.x

Purcell, S. M., Moran, J. L., Fromer, M., Ruderfer, D., Solovieff, N., Roussos, P., . . . Sklar, P. (2014). A polygenic burden of rare disruptive mutations in schizophrenia. *Nature, 506*(7487), 185-190. doi:10.1038/nature12975

Rabiner, C. A., Mains, R. E., & Eipper, B. A. (2005). Kalirin: a dual Rho guanine nucleotide exchange factor that is so much more than the sum of its many parts. *Neuroscientist, 11*(2), 148-160. doi:11/2/148 [pii]

10.1177/1073858404271250

Rapoport, J. L., Giedd, J. N., Blumenthal, J., Hamburger, S., Jeffries, N., Fernandez, T., . . . Evans, A. (1999). Progressive cortical change during adolescence in childhood-onset schizophrenia. A longitudinal magnetic resonance imaging study. *Arch Gen Psychiatry, 56*(7), 649-654.

Remmers, C., Sweet, R. A., & Penzes, P. (2014). Abnormal kalirin signaling in neuropsychiatric disorders. *Brain Research Bulletin, 103*, 29-38. doi:10.1016/j.brainresbull.2013.12.006

Ripke, S., O'Dushlaine, C., Chambert, K., Moran, J. L., Kahler, A. K., Akterin, S., . . . Sullivan, P. F. (2013). Genome-wide association analysis identifies 13 new risk loci for schizophrenia. *Nat Genet, 45*(10), 1150-1159. doi:10.1038/ng.2742

Rosoklija, G., Toomayan, G., Ellis, S. P., Keilp, J., Mann, J. J., Latov, N., . . . Dwork, A. J. (2000). Structural abnormalities of subicular dendrites in subjects with schizophrenia and mood disorders: preliminary findings. *Arch Gen Psychiatry, 57*(4), 349-356.

Rubio, M. D., Haroutunian, V., & Meador-Woodruff, J. H. (2012). Abnormalities of the Duo/Ras-

related C3 botulinum toxin substrate 1/p21-activated kinase 1 pathway drive myosin light chain phosphorylation in frontal cortex in schizophrenia. *Biological Psychiatry, 71*(10), 906-914. doi:http://dx.doi.org/10.1016/j.biopsych.2012.02.006

Rutkowski, T. P., Schroeder, J. P., Gafford, G. M., Warren, S. T., Weinshenker, D., Caspary, T., & Mulle, J. G. (2016). Unraveling the genetic architecture of copy number variants associated with schizophrenia and other neuropsychiatric disorders. *J Neurosci Res*. doi:10.1002/jnr.23970

Sadybekov, A., Tian, C., Arnesano, C., Katritch, V., & Herring, B. E. (2017). An autism spectrum disorder-related de novo mutation hotspot discovered in the GEF1 domain of Trio. *Nat Commun, 8*(1), 601. doi:10.1038/s41467-017-00472-0

Saha, S., Chant, D., & McGrath, J. (2007). A systematic review of mortality in schizophrenia: is the differential mortality gap worsening over time? *Arch Gen Psychiatry, 64*(10), 1123-1131. doi:10.1001/archpsyc.64.10.1123

Schizophrenia Working Group of the Psychiatric Genomics Consortium. (2014). Biological insights from 108 schizophrenia-associated genetic loci. *Nature, 511*(7510), 421-427. doi:10.1038/nature13595

Schneider, C. A., Rasband, W. S., & Eliceiri, K. W. (2012). NIH Image to ImageJ: 25 years of image analysis. *Nat Methods, 9*(7), 671-675.

Sebat, J., Levy, D. L., & McCarthy, S. E. (2009). Rare structural variants in schizophrenia: one disorder, multiple mutations; one mutation, multiple disorders. *Trends Genet, 25*(12), 528-535. doi:S0168-9525(09)00202-9 [pii]

10.1016/j.tig.2009.10.004

Selemon, L. D., & Goldman-Rakic, P. S. (1999). The reduced neuropil hypothesis: a circuit based

model of schizophrenia. *Biol Psychiatry, 45*(1), 17-25. doi:S0006-3223(98)00281-9 [pii]

Selemon, L. D., Rajkowska, G., & Goldman-Rakic, P. S. (1998). Elevated neuronal density in prefrontal area 46 in brains from schizophrenic patients: application of a three-dimensional, stereologic counting method. *J Comp Neurol, 392*(3), 402-412. doi:10.1002/(SICI)1096-9861(19980316)392:3<402::AID-CNE9>3.0.CO;2-5 [pii]

Sham, P. C., MacLean, C. J., & Kendler, K. S. (1994). A typological model of schizophrenia based on age at onset, sex and familial morbidity. *Acta Psychiatr Scand, 89*(2), 135-141.

Silveira, J. M., & Seeman, M. V. (1995). Shared psychotic disorder: a critical review of the literature. *Can J Psychiatry, 40*(7), 389-395.

Soderling, S. H., Guire, E. S., Kaech, S., White, J., Zhang, F., Schutz, K., . . . Scott, J. D. (2007). A WAVE-1 and WRP signaling complex regulates spine density, synaptic plasticity, and memory. *J Neurosci, 27*(2), 355-365. doi:10.1523/JNEUROSCI.3209-06.2006

Steen, R. G., Mull, C., McClure, R., Hamer, R. M., & Lieberman, J. A. (2006). Brain volume in first-episode schizophrenia: systematic review and meta-analysis of magnetic resonance imaging studies. *Br J Psychiatry, 188*, 510-518. doi:188/6/510 [pii]

10.1192/bjp.188.6.510

Suddath, R. L., Casanova, M. F., Goldberg, T. E., Daniel, D. G., Kelsoe, J. R., Jr., & Weinberger, D. R. (1989). Temporal lobe pathology in schizophrenia: a quantitative magnetic resonance imaging study. *Am J Psychiatry, 146*(4), 464-472. doi:10.1176/ajp.146.4.464

Sullivan, P. F., Daly, M. J., & O'Donovan, M. (2012). Genetic architectures of psychiatric disorders: the emerging picture and its implications. *Nat Rev Genet, 13*(8), 537-551. doi:10.1038/nrg3240

Sullivan, P. F., Lin, D., Tzeng, J. Y., van den Oord, E., Perkins, D., Stroup, T. S., . . . Close, S. L.

(2008). Genomewide association for schizophrenia in the CATIE study: results of stage 1. *Mol Psychiatry, 13*(6), 570-584. doi:10.1038/mp.2008.25

Sweet, R. A., Henteleff, R. A., Zhang, W., Sampson, A. R., & Lewis, D. A. (2009). Reduced dendritic spine density in auditory cortex of subjects with schizophrenia. *Neuropsychopharmacology, 34*(2), 374-389. doi:10.1038/npp.2008.67

Thompson, P. M., Vidal, C., Giedd, J. N., Gochman, P., Blumenthal, J., Nicolson, R., . . . Rapoport, J. L. (2001). Mapping adolescent brain change reveals dynamic wave of accelerated gray matter loss in very early-onset schizophrenia. *Proc Natl Acad Sci U S A, 98*(20), 11650-11655. doi:10.1073/pnas.201243998

98/20/11650 [pii]

Tolias, K. F., Duman, J. G., & Um, K. (2011). Control of synapse development and plasticity by Rho GTPase regulatory proteins. *Prog Neurobiol, 94*(2), 133-148. doi:10.1016/j.pneurobio.2011.04.011

Tosato, S., Bellani, M., Bonetto, C., Ruggeri, M., Perlini, C., Lasalvia, A., . . . Brambilla, P. (2012). Is neuregulin 1 involved in determining cerebral volumes in schizophrenia? Preliminary results showing a decrease in superior temporal gyrus volume. *Neuropsychobiology, 65*(3), 119-125. doi:10.1159/000330584

Vanleeuwen, J. E., & Penzes, P. (2012). Long-term perturbation of spine plasticity results in distinct impairments of cognitive function. *J Neurochem, 123*(5), 781-789. doi:10.1111/j.1471-4159.2012.07899.x

Vita, A., De Peri, L., Deste, G., & Sacchetti, E. (2012). Progressive loss of cortical gray matter in schizophrenia: a meta-analysis and meta-regression of longitudinal MRI studies. *Transl Psychiatry, 2*, e190. doi:10.1038/tp.2012.116

tp2012116 [pii]

Walker, E., Kestler, L., Bollini, A., & Hochman, K. M. (2004). Schizophrenia: etiology and course. *Annu Rev Psychol, 55*, 401-430. doi:10.1146/annurev.psych.55.090902.141950

Wang, L., Hauser, E. R., Shah, S. H., Pericak-Vance, M. A., Haynes, C., Crosslin, D., . . . Vance, J. M. (2007). Peakwide mapping on chromosome 3q13 identifies the kalirin gene as a novel candidate gene for coronary artery disease. *Am J Hum Genet, 80*(4), 650-663. doi:10.1086/512981

Wang, M., Li, H., Takumi, T., Qiu, Z., Xu, X., Yu, X., & Bian, W. J. (2017). Distinct Defects in Spine Formation or Pruning in Two Gene Duplication Mouse Models of Autism. *Neurosci Bull, 33*(2), 143-152. doi:10.1007/s12264-017-0111-8

Ward-Caviness, C., Haynes, C., Blach, C., Dowdy, E., Gregory, S. G., Shah, S. H., . . . Hauser, E. R. (2013). Gene-smoking interactions in multiple Rho-GTPase pathway genes in an early-onset coronary artery disease cohort. *Hum Genet, 132*(12), 1371-1382. doi:10.1007/s00439-013-1339-7

Warde-Farley, D., Donaldson, S. L., Comes, O., Zuberi, K., Badrawi, R., Chao, P., . . . Morris, Q. (2010). The GeneMANIA prediction server: biological network integration for gene prioritization and predicting gene function. *Nucleic Acids Res, 38*(Web Server issue), W214-220. doi:10.1093/nar/gkq537

Wegner, A. M., Nebhan, C. A., Hu, L., Majumdar, D., Meier, K. M., Weaver, A. M., & Webb, D. J. (2008). N-wasp and the arp2/3 complex are critical regulators of actin in the development of dendritic spines and synapses. *J Biol Chem, 283*(23), 15912-15920. doi:10.1074/jbc.M801555200

Wei, Q., Wang, L., Wang, Q., Kruger, W. D., & Dunbrack, R. L., Jr. (2010). Testing computational

prediction of missense mutation phenotypes: functional characterization of 204 mutations of human cystathionine beta synthase. *Proteins, 78*(9), 2058-2074. doi:10.1002/prot.22722

Weinberger, D. R., Berman, K. F., & Zec, R. F. (1986). Physiologic dysfunction of dorsolateral prefrontal cortex in schizophrenia. I. Regional cerebral blood flow evidence. *Arch Gen Psychiatry, 43*(2), 114-124.

Woolfrey, K. M., Srivastava, D. P., Photowala, H., Yamashita, M., Barbolina, M. V., Cahill, M. E., . . . Penzes, P. (2009). Epac2 induces synapse remodeling and depression and its disease-associated forms alter spines. *Nat Neurosci, 12*(10), 1275-1284. doi:nn.2386 [pii] 10.1038/nn.2386

Xie, Z., Cahill, M. E., & Penzes, P. (2010). Kalirin loss results in cortical morphological alterations. *Mol Cell Neurosci, 43*(1), 81-89. doi:10.1016/j.mcn.2009.09.006

Xie, Z., Cahill, M. E., Radulovic, J., Wang, J., Campbell, S. L., Miller, C. A., . . . Penzes, P. (2011). Hippocampal phenotypes in kalirin-deficient mice. *Mol Cell Neurosci, 46*(1), 45-54. doi:10.1016/j.mcn.2010.08.005

Xie, Z., Srivastava, D. P., Photowala, H., Kai, L., Cahill, M. E., Woolfrey, K. M., . . . Penzes, P. (2007). Kalirin-7 controls activity-dependent structural and functional plasticity of dendritic spines. *Neuron, 56*(4), 640-656. doi:10.1016/j.neuron.2007.10.005

Xin, X., Rabiner, C. A., Mains, R. E., & Eipper, B. A. (2009). Kalirin12 interacts with dynamin. *BMC Neuroscience, 10*, 61. doi:10.1186/1471-2202-10-61

Yan, Z., Kim, E., Datta, D., Lewis, D. A., & Soderling, S. H. (2016). Synaptic Actin Dysregulation, a Convergent Mechanism of Mental Disorders? *J Neurosci, 36*(45), 11411-11417. doi:10.1523/JNEUROSCI.2360-16.2016

Zipursky, R. B., Lim, K. O., Sullivan, E. V., Brown, B. W., & Pfefferbaum, A. (1992). Widespread

cerebral gray matter volume deficits in schizophrenia. *Arch Gen Psychiatry, 49*(3), 195-205.

Zuker, M. (2003). Mfold web server for nucleic acid folding and hybridization prediction. *Nucleic Acids Res, 31*(13), 3406-3415.